CSIAM Trans. Appl. Math.
doi: 10.4208/csiam-am.SO-2024-0012

Vol. **6**, No. 1, pp. 176-206
March 2025

Stochastic Runge-Kutta Methods for Preserving Maximum Bound Principle of Semilinear Parabolic Equations. Part II: Sinc Quadrature Rule

Yabing Sun[1] and Weidong Zhao[2,*]

[1] *College of Science, National University of Defense Technology, Changsha 410073, China.*
[2] *School of Mathematics, Shandong University, Jinan 250100, China.*

Received 23 April 2024; Accepted 23 November 2024

Abstract. The maximum bound principle (MBP) is an important property for a large class of semilinear parabolic equations. To propose MBP-preserving schemes with high spatial accuracy, in the first part of this series, we developed a class of time semidiscrete stochastic Runge-Kutta (SRK) methods for semilinear parabolic equations, and constructed the first- and second-order fully discrete MBP-preserving SRK schemes. In this paper, to develop higher order fully discrete MBP-preserving SRK schemes with spectral accuracy in space, we use the Sinc quadrature rule to approximate the conditional expectations in the time semidiscrete SRK methods and propose a class of fully discrete MBP-preserving SRK schemes with up to fourth-order accuracy in time for semilinear equations. Based on the property of the Sinc quadrature rule, we theoretically prove that the proposed fully discrete SRK schemes preserve the MBP and can achieve an exponential order convergence rate in space. In addition, we reveal that the conditional expectation with respect to the Bronwian motion in the time semidiscrete SRK method is essentially equivalent to the exponential Laplacian operator under the periodic boundary condition. Ample numerical experiments are also performed to demonstrate our theoretical results and to show the exponential order convergence rate in space of the proposed schemes.

AMS subject classifications: 35B50, 60H30, 65L06, 65M12, 65M75

Key words: Semilinear parabolic equation, stochastic Runge-Kutta scheme, Sinc quadrature rule, MBP-preserving, exponential convergence rate.

1 Introduction

Consider the following initial-boundary-value problem of a semilinear parabolic partial differential equation (PDE) in the backward form:

*Corresponding author. *Email addresses:* sunybly@163.com (Y. Sun), wdzhao@sdu.edu.cn (W. Zhao)

$$
\begin{aligned}
&u_t+\frac{1}{2}\sigma\sigma^\top:\nabla^2 u+f(u)=0, && (t,\boldsymbol{x})\in[0,T)\times D,\\
&u(t,\cdot) \text{ is } D\text{-periodic}, && t\in[0,T],\\
&u(T,\boldsymbol{x})=\varphi(\boldsymbol{x}), && \boldsymbol{x}\in\overline{D},
\end{aligned}
\tag{1.1}
$$

where $u(t,\boldsymbol{x})$ denotes the unknown function, $D=(0,a)^d\subset\mathbb{R}^d$ $(d=1,2,3)$ is a hypercube domain, f is a nonlinear operator, and the matrix $\sigma\in\mathbb{R}^{d\times d}$ is defined as

$$
\sigma=\begin{pmatrix}\sigma_1 & & & \\ & \sigma_2 & & \\ & & \ddots & \\ & & & \sigma_d\end{pmatrix},\quad \sigma_i\neq 0,\quad i=1,\ldots,d.
$$

It is well known that the semilinear parabolic equation (1.1) possesses the MBP in the sense that the absolute value of its solution is pointwise bounded for all time by some specific constant under appropriate initial and/or boundary conditions [9]. Up to now, great efforts have been made in developing MBP-preserving numerical methods for equations like (1.1). For the temporal discretizations, one is referred to [8–15, 18–20, 22–24, 26, 27, 33, 36, 41] and references therein. As for the spatial discretizations, a partial list of earlier works includes [2–6, 16, 17, 22, 30, 31, 37, 39, 40, 42]. Recently, the authors in [7] studied the effect of noise on the MBP-preserving property and energy evolution property of numerical methods for stochastic parabolic partial differential equation with a logarithmic Flory-Huggins potential.

Since the spectral method can not be used to construct the MBP-preserving numerical schemes for the equations like (1.1), to improve the efficiency of the long time simulations, it is important and necessary to develop some MBP-preserving schemes for (1.1) with high spatial accuracy.

In the first part of this series [35], we developed a first-order and a second-order SRK schemes with high spatial accuracy based on the probabilistic representation of the solution of (1.1) via the backward stochastic differential equation (BSDE) [29,32]. The key idea is to represent the solution of (1.1) as an integral equation via BSDE, which contains only some conditional expectations with respect to a diffusion process but not any differential operator. By applying the classical Runge-Kutta method to this integral equation, we developed a class of time semidiscrete MBP-preserving SRK methods up to fourth-order for (1.1). Since the diffusion process is a Gaussian process, one can write the conditional expectation as an integral with respect to a negative exponential function. Then we further constructed the first- and second-order fully discrete MBP-preserving SRK schemes by using the three-point Gauss-Hermite quadrature rule to approximate the integrals in the time semidiscrete schemes. Assuming that Δt is the temporal step size and $\sigma_i=\sigma_0$ for $i=1,\ldots,d$, our error analysis shows that the spatial errors of the proposed schemes in maximum norm are proportional to $\sigma_0^6\Delta t^2$ and thus can be neglected compared with the temporal errors especially for the small values of σ_0.

As shown in the first part [35], when using the Gauss-Hermite quadrature rule to approximate the conditional expectations, we can only obtain the fully discrete MBP-preserving SRK schemes with up to second-order accuracy in time. The main reason is that we need to avoid using the interpolation when constructing the fully discrete MBP-preserving schemes with high spatial accuracy, since only linear interpolation can preserve the MBP. Because the Gauss-Hermite quadrature points are fixed and nonuniform, we can only choose the three-point Gauss-Hermite quadrature rule to approximate the conditional expectations in the first- and second-order time semidiscrete SRK methods to construct the fully discrete MBP-preserving SRK schemes without using the interpolation. To construct the fully discrete MBP-preserving SRK schemes with higher order accuracy in time and exponential order accuracy in space, in this paper, we shall adopt the Sinc quadrature rule [38] to approximate the conditional expectations in the time semidiscrete SRK methods developed in [35]. Specifically, we propose a class of fully discrete MBP-preserving SRK schemes with up to fourth-order accuracy in time and exponential order accuracy in space by using the Sinc quadrature rule to approximate conditional expectations in the semidiscrete schemes. By combining with the property of the Sinc quadrature rule, we prove the preservation of MBP of the proposed fully discrete SRK schemes under some reasonable assumptions. We also rigourously establish their error estimates, which show that the spatial errors of the schemes decrease in an exponential speed with respect to the number of quadrature points M. In fact, if we set the temporal and spatial step sizes Δt and Δx to satisfy $2\Delta x = \sigma_0\sqrt{\Delta t}$, the spatial errors of the schemes are proportional to $\exp(-M^2/8)/\Delta t$. Besides, since all the coefficient matrices of the proposed fully discrete schemes are circular, they can be implemented efficiently via the fast fourier transform (FFT) technique. As far as we know, this is the first attempt to design the fully discrete MBP-preserving schemes with exponential order convergence rate in space for the semilinear parabolic equations.

Compared with the ones developed in the first part [35], the fully discrete MBP-preserving SRK schemes proposed in this paper can achieve higher order convergence rates in time and an exponential order convergence rate in space. Now we note the main advantages of the proposed fully discrete SRK schemes.

The fully discrete SRK schemes possess high spatial accuracy as well as simple structure. Specifically, the spatial errors of the fully discrete schemes behave like the ones of the spectral method with an exponential order convergence rate, whilst their coefficient matrices are simple as the ones of the central difference method used in other classic MBP-preserving schemes, which are symmetric and circular.

In addition, by analyzing their eigenvalues, we show that the conditional expectation with respect to the Brownian motion is essentially equivalent to the exponential Laplacian operator under the periodic boundary condition in the sense that they have exactly the same eigenvalues. In other words, we can provide an integral representation for the exponential Laplacian differential operator. Moreover, by replacing the conditional expectations in the time semidiscrete SRK schemes with the corresponding exponential Laplacian operators, we obtain the time semidiscrete integrating factor Runge-

Kutta (IFRK) schemes. Thus, the time semidiscrete SRK and IFRK schemes are essentially equivalent to each other. However, the totally different ways of discretizations for the two different types of operators lead to totally different fully discrete SRK and IFRK schemes.

The rest of the paper is organized as follows. In Section 2, we briefly review the probabilistic representation of the solution of (1.1) via BSDE and derive its MBP via the comparison theorem of BSDE. Based on this representation, we introduce the time semidiscrete SRK method developed in [35] and discuss its equivalence to the time semidiscrete IFRK method in Section 3. In Section 4, by using the Sinc quadrature rule to approximate the conditional expectations in the time semidiscrete SRK method, we propose a class of fully discrete MBP-preserving SRK schemes, establish their error estimates and construct some specific SRK schemes with up to fourth-order temporal accuracy. In Section 5, we carry out various numerical experiments to verify the convergence and the MBP preservation of the proposed schemes. Some concluding remarks are finally given in Section 6.

2 The probabilistic interpretation of semilinear PDE

As shown in [35], one of the key ingredients to develop the SRK scheme is the representation of the solution of (1.1) via BSDE. To give such representation, we let $\mathbb{F}=(\mathcal{F}_t)_{0\le t\le T}$ be the filtration generated by a d-dimensional Brownian motion $W=(W_t)_{0\le t\le T}$ and consider the BSDE defined on the filtered complete probability space $(\Omega,\mathcal{F},\mathbb{F},P)$ as below

$$Y_t=\varphi(X_T)+\int_t^T f(Y_r)dr-\int_t^T Z_r dW_r, \quad 0\le t\le T, \tag{2.1}$$

where $X_t=X_0+\sigma W_t$ is a d-dimensional diffusion process with $X_0\in\mathcal{F}_0$ being the initial condition. A couple (Y_t,Z_t) is called an L^2-adapted solution of the BSDE (2.1) if it is $\mathcal{F}_t$-adapted, square integrable and satisfies (2.1).

Now we show the relationship between the solutions of (1.1) and (2.1) in the following lemma [32].

Lemma 2.1. *Assume that the functions f and φ are Lipschitz continuous, then the BSDE* (2.1) *admits a unique adapted solution (Y_t,Z_t) and the viscosity solution of the PDE* (1.1) *can be represented as*

$$u(t,\boldsymbol{x})=Y_t^{t,\boldsymbol{x}}, \tag{2.2}$$

where $Y_t^{t,\boldsymbol{x}}$ is the value of Y_t with X_t starting from $(t,\boldsymbol{x})$. Conversely, if u is the classical solution of the PDE (1.1)*, then the adapted solution of the BSDE* (2.1) *can be represented as*

$$Y_t=u(t,X_t), \quad Z_t=(\nabla u\sigma)(t,X_t), \tag{2.3}$$

which are the so called nonlinear Feynman-Kac formula.

The above lemma indicates that the MBP of the solution of (1.1) is a direct result of the following comparison theorem for BSDE.

Theorem 2.1 (Comparison Theorem, [21]). *Let* (Y_t^i, Z_t^i) *for* $i=1,2$ *be the solutions of the following BSDEs:*

$$Y_t^i = \xi^i + \int_t^T f^i(Y_r^i)dr - \int_t^T Z_r^i dW_r, \quad 0 \le t \le T,$$

respectively, where the functions $f^i : \mathbb{R} \to \mathbb{R}$ *are Lipschitz continuous and the terminal conditions* $\xi^i \in \mathcal{F}_T$ *are square integrable random variables. Then if almost surely*

$$\xi^1 \ge \xi^2, \quad f^1(Y_t^2) \ge f^2(Y_t^2),$$

we have that almost surely for any time $t \in [0,T], Y_t^1 \ge Y_t^2$.

Theorem 2.2 (Maximum Bound Principle, [35]). *Assume that* f *and* φ *are Lipschitz continuous and there exists a positive constant* ρ *such that*

$$f(\rho) = f(-\rho) = 0.$$

Then if $-\rho \le \varphi(\boldsymbol{x}) \le \rho$ *for any* $\boldsymbol{x} \in \overline{D}$, *the classical solution* $u(t,\boldsymbol{x})$ *of* (1.1) *satisfies*

$$-\rho \le u(t,\boldsymbol{x}) \le \rho, \quad \forall (t,\boldsymbol{x}) \in [0,T] \times \overline{D}.$$

Remark 2.1. We point out that under the monotonicity assumption on f, the Lipschitz condition on f in Lemma 2.1 can be weakened to the polynomial growth [1] and to an arbitrary growth [28]. On the other hand, when f and φ are smooth enough, the viscosity solution u in Lemma 2.1 becomes the classical solution. In fact, if $f \in C_b^{2+2k}$ and $\varphi \in C_b^{2+2k+\alpha}$ for an $\alpha \in (0,1)$, we have [43]

$$u \in C_b^{1+k,2+2k}, \quad k = 0,1,2,\ldots,$$

where C_b^l is the set of continuous differential functions $\phi(\boldsymbol{x})$ with uniformly bounded partial derivatives up to the l-th order and $C_b^{l+\alpha}$ is the set of functions in C_b^l whose l-th order derivative is Hölder continuous with index α.

Remark 2.2. The condition $f(\rho) = f(-\rho) = 0$ in Theorem 2.2 is satisfied by many semilinear parabolic equations such as the Allen-Cahn equation, where $f(u)$ usually takes the following two forms:

$$f(u) = \begin{cases} u - u^3, & \text{Ginzburg-Landau potential}, \\ \dfrac{\theta}{2}\ln\dfrac{1-u}{1+u} + \theta_c u, & \text{Flory-Huggins potential}. \end{cases} \tag{2.4}$$

Thus, it is obvious that $\rho = 1$ for the Ginzburg-Landau potential. As for the Flory-Huggins potential, we take $\theta = 0.8$ and $\theta_c = 1.6$ to obtain $\rho \approx 0.9575$.

3 The time semidiscrete SRK schemes

In this section, we recall the time semidiscrete SRK method for solving (1.1) proposed in [35] and discuss its relationship with the integrating factor Runge-Kutta method. To this end, we introduce the following uniform time partition:

$$t_n = n\Delta t, \quad n = 0,1,\ldots,N_t,$$

where $\Delta t = T/N_t$ with N_t being a given positive integer. For a positive integer s, let $\{a_{ij}, i,j = 0,\ldots,s\}$ and $\{c_i, i = 0,\ldots,s\}$ be real numbers satisfying $a_{ij} = 0$ for $i \leq j$ and

$$\begin{aligned} &0 = c_0 \leq \cdots \leq c_s = 1, \\ &\sum_{j=0}^{i-1} a_{ij} = c_i, \quad i = 0,\ldots,s. \end{aligned} \tag{3.1}$$

Then we define the s intermediate times in $[t_n, t_{n+1}]$ as

$$t_n^i = t_{n+1} - c_i \Delta t, \quad i = 0,\ldots,s,$$

and thus $t_n = t_n^s \leq \cdots \leq t_n^0 = t_{n+1}$.

3.1 The time semidiscrete schemes

To develop the time semidiscrete SRK scheme, for $n = 0,\ldots,N_t - 1$, we write (2.1) as

$$Y_t = Y_{t_{n+1}} + \int_t^{t_{n+1}} f(Y_r)dr - \int_t^{t_{n+1}} Z_r dW_r, \quad 0 \leq t \leq t_{n+1}. \tag{3.2}$$

Then by inserting the formula (2.3) into (3.2), we obtain

$$u(t,X_t) = u(t_{n+1}, X_{t_{n+1}}) + \int_t^{t_{n+1}} f\big(u(r,X_r)\big)dr - \int_t^{t_{n+1}} (\nabla u \sigma)(r,X_r)dW_r, \tag{3.3}$$

where u is the classical solution of (1.1). Let $\mathcal{M}_t$ be the σ-algebra generated by $(X_r)_{0 \leq r \leq t}$ and take the conditional expectation $\mathbb{E}_t^{X_t}[\cdot] = \mathbb{E}\big[\cdot|\mathcal{M}_t\big]$ on both sides of the Eq. (3.3), and we have the following integral equation:

$$u(t,X_t) = \mathbb{E}_t^{X_t}[u(t_{n+1}, X_{t_{n+1}})] + \int_t^{t_{n+1}} \mathbb{E}_t^{X_t}\big[f\big(u(r,X_r)\big)\big]dr. \tag{3.4}$$

Thus, by taking $t = t_n^i$ in (3.4), we deduce the following reference equations:

$$\bar{u}\big(t_n^i, X_{t_n^i}\big) = \mathbb{E}_{t_n^i}^{X_{t_n^i}}[u(t_{n+1}, X_{t_{n+1}})] + \Delta t \sum_{j=0}^{i-1} a_{ij} \mathbb{E}_{t_n^i}^{X_{t_n^i}}\big[f\big(\bar{u}\big(t_n^j, X_{t_n^j}\big)\big)\big], \quad i = 0,\ldots,s-1, \tag{3.5}$$

$$u(t_n,X_{t_n})=\mathbb{E}_{t_n}^{X_{t_n}}[u(t_{n+1},X_{t_{n+1}})]+\Delta t\sum_{i=0}^{s-1}a_{si}\mathbb{E}_{t_n}^{X_{t_n}}\left[f\left(\bar{u}\left(t_n^i,X_{t_n^i}\right)\right)\right]+R_n, \tag{3.6}$$

where $\bar{u}(t_n^0,X_{t_n^0})=u(t_{n+1},X_{t_{n+1}})$ for $i=0$ and R_n is the local truncation error.

Let $u_n(\boldsymbol{x})$ and $u_n^{(i)}(\boldsymbol{x})$ be the approximations for the solution $u(t,\boldsymbol{x})$ of (1.1) at times t_n and t_n^i, respectively. Then we take $X_{t_n^i}=\boldsymbol{x}$ in (3.5) and (3.6) to get explicit time semidiscrete s-stage SRK scheme for solving (1.1) in Butcher form

$$\begin{aligned}
&u_n^{(0)}(\boldsymbol{x})=u_{n+1}(\boldsymbol{x}),\\
&u_n^{(i)}(\boldsymbol{x})=\mathbb{E}_{t_n^i}^{\boldsymbol{x}}\left[u_{n+1}(X_{t_{n+1}})+\Delta t\sum_{j=0}^{i-1}a_{ij}f\left(u_n^{(j)}\left(X_{t_n^j}\right)\right)\right], \quad i=1,\ldots,s,\\
&u_n(\boldsymbol{x})=u_n^{(s)}(\boldsymbol{x}).
\end{aligned}$$

By using the conditional expectation property, we derive its Shu-Osher form [35]

$$\begin{aligned}
&u_n^{(0)}(\boldsymbol{x})=u_{n+1}(\boldsymbol{x}),\\
&u_n^{(i)}(\boldsymbol{x})=\sum_{j=0}^{i-1}\mathbb{E}_{t_n^i}^{\boldsymbol{x}}\left[\alpha_{ij}u_n^{(j)}\left(X_{t_n^j}\right)+\Delta t\beta_{ij}f\left(u_n^{(j)}\left(X_{t_n^j}\right)\right)\right], \quad i=1,\ldots,s,\\
&u_n(\boldsymbol{x})=u_n^{(s)}(\boldsymbol{x}),
\end{aligned}$$

where the coefficients $\{\alpha_{ij}\}$ and $\{\beta_{ij}\}$ satisfy $\alpha_{ij}\geq 0$ for $i,j=1,2,\ldots,s$ and

$$\sum_{j=0}^{i-1}\alpha_{ij}=1, \quad \beta_{ij}=a_{ij}-\sum_{k=j+1}^{i-1}\alpha_{ik}a_{kj}, \quad i=1,\ldots,s.$$

Moreover, for a measurable function $g:\mathbb{R}^d\rightarrow\mathbb{R}$, it holds that

$$\mathbb{E}_t^{\boldsymbol{x}}[g(X_r)]=\mathbb{E}\left[g\left(X_r^{t,\boldsymbol{x}}\right)\right], \quad 0\leq t\leq r\leq T,$$

where

$$X_r^{t,\boldsymbol{x}}=\boldsymbol{x}+\sigma(W_r-W_t). \tag{3.7}$$

Now we get the time semidiscrete s-stage SRK scheme for solving (1.1) as

$$\begin{aligned}
&u_n^{(0)}(\boldsymbol{x})=u_{n+1}(\boldsymbol{x}),\\
&u_n^{(i)}(\boldsymbol{x})=\sum_{j=0}^{i-1}\mathbb{E}\left[\alpha_{ij}u_n^{(j)}\left(X_{t_n^j}^{t_n^i,\boldsymbol{x}}\right)+\Delta t\beta_{ij}f\left(u_n^{(j)}\left(X_{t_n^j}^{t_n^i,\boldsymbol{x}}\right)\right)\right], \quad i=1,\ldots,s,\\
&u_n(\boldsymbol{x})=u_n^{(s)}(\boldsymbol{x}).
\end{aligned} \tag{3.8}$$

To show the MBP-preserving property and error estimate of the time semidiscrete SRK scheme (3.8), we assume that the nonlinear term satisfies

$$\exists r_0^+ > 0 \quad \text{such that} \quad |\xi + rf(\xi)| \le \rho, \quad \forall \xi \in [-\rho,\rho], \quad \forall r \in (0, r_0^+], \tag{3.9}$$

$$\exists r_0^- > 0 \quad \text{such that} \quad |\xi - rf(\xi)| \le \rho, \quad \forall \xi \in [-\rho,\rho], \quad \forall r \in (0, r_0^-]. \tag{3.10}$$

Besides, we assume that α_{ij} is zero only if its corresponding β_{ij} is zero. Then we have the following MBP-preserving property [35].

Theorem 3.1. *Assume that f satisfies* (3.9) *and* (3.10)*, then if $\|u_{n+1}\|_{L^\infty} \le \rho$, the solution u_n obtained from* (3.8) *satisfies $\|u_n\|_{L^\infty} \le \rho$, provided that*

$$\Delta t \le \mathcal{C} r_0^+, \quad \mathcal{C} = \min_{i,j} \frac{\alpha_{ij}}{\beta_{ij}}, \tag{3.11}$$

when β_{ij} are all nonnegative, or satisfies

$$\Delta t \le \mathcal{C} \min\{r_0^+, r_0^-\}, \quad \mathcal{C} = \min_{i,j} \frac{\alpha_{ij}}{|\beta_{ij}|}, \tag{3.12}$$

whenever there is a negative β_{ij}.

Suppose the SRK scheme (3.8) is p-th order accurate with $1 \le p \le s$ and we have the following error estimate [35].

Theorem 3.2. *Let u_n be the solution obtained from* (3.8) *with $u_{N_t}(\boldsymbol{x}) = \varphi(\boldsymbol{x})$. Assume that $\|\varphi\|_{L^\infty} \le \rho$ and the exact solution u of* (1.1) *satisfies $u \in C_b^{p+1,2p+2}$. Then under the conditions in Theorem* 3.1*, we get*

$$\|u(t_n,\cdot) - u_n\|_{L^\infty} \le C_1 \left(e^{\tilde{C}s(T-t_n)} - 1\right) (\Delta t)^p, \quad n = 0, \ldots, N_t,$$

where $\tilde{C} = \max_{|\xi| \le \rho} |f'(\xi)|$ and the positive constant C_1 is independent of Δt.

Remark 3.1. We take the Allen-Cahn equation for instance to illustrate the conditions (3.9) and (3.10). For the Ginzburg-Landau potential, we have [20]

$$r_0^+ = \frac{1}{2}, \quad r_0^- = 1, \tag{3.13}$$

and for the Flory-Huggins potential, we have

$$r_0^+ = \frac{1-\rho^2}{\theta - \theta_c(1-\rho^2)}, \quad r_0^- = \frac{1}{\theta_c - \theta}. \tag{3.14}$$

Remark 3.2. Note that the sufficient conditions to preserve the MBP for the SRK schemes in Theorem 3.1 are the same as the ones for the IFRK schemes proposed in [20]. Thus, one can construct some specific time semidiscrete MBP-preserving SRK schemes with up to fourth-order accuracy by choosing exactly the same coefficients of the MBP-preserving IFRK schemes as given in [20].

3.2 The relationship with the IFRK schemes

We first recall the time semidiscrete s-stage IFRK scheme for solving (1.1) proposed in [20] as below

$$
\begin{aligned}
&u_n^{(0)}(\boldsymbol{x}) = u_{n+1}(\boldsymbol{x}),\\
&u_n^{(i)}(\boldsymbol{x}) = \sum_{j=0}^{i-1} e^{(c_i-c_j)\Delta t\mathcal{L}}\left[\alpha_{ij}u_n^{(j)}(\boldsymbol{x}) + \Delta t\beta_{ij} f\left(u_n^{(j)}(\boldsymbol{x})\right)\right], \quad i=1,\ldots,s,\\
&u_n(\boldsymbol{x}) = u_n^{(s)}(\boldsymbol{x}),
\end{aligned}
\tag{3.15}
$$

where $\mathcal{L}$ is the linear operator in (1.1), that is,

$$
\mathcal{L} = \frac{1}{2}\sigma\sigma^\top : \nabla^2 = \frac{1}{2}\sum_{l=1}^{d}\sigma_l^2\partial_{x_l x_l}^2.
$$

To reveal the relationship between the time semidiscrete SRK and IFRK schemes, for a given function $g:\mathbb{R}^d \to \mathbb{R}$, we define the following conditional expectation operators:

$$
\tilde{\mathbb{E}}_{c_i,c_j,\Delta t}[g(\boldsymbol{x})] := \mathbb{E}_{t_n^i}^{\boldsymbol{x}}\left[g\left(X_{t_n^j}\right)\right] = \mathbb{E}\left[g\left(X_{t_n^j}^{t_n^i,\boldsymbol{x}}\right)\right], \quad 0 \le j \le i \le s.
$$

Then the time semidiscrete s-stage SRK scheme (3.8) can be written as

$$
\begin{aligned}
&u_n^{(0)}(\boldsymbol{x}) = u_{n+1}(\boldsymbol{x}),\\
&u_n^{(i)}(\boldsymbol{x}) = \sum_{j=0}^{i-1} \tilde{\mathbb{E}}_{c_i,c_j,\Delta t}\left[\alpha_{ij}u_n^{(j)}(\boldsymbol{x}) + \Delta t\beta_{ij} f\left(u_n^{(j)}(\boldsymbol{x})\right)\right], \quad i=1,\ldots,s,\\
&u_n(\boldsymbol{x}) = u_n^{(s)}(\boldsymbol{x}).
\end{aligned}
\tag{3.16}
$$

By comparing (3.15) and (3.16), we observe that the s-stage SRK and IFRK schemes have exactly the same form except that the exponential Laplacian operator $e^{(c_i-c_j)\Delta t\mathcal{L}}$ in (3.15) is replaced by the conditional expectation operator $\tilde{\mathbb{E}}_{c_i,c_j,\Delta t}$ in (3.16). Thus, one natural question is:

- What is the relationship between the exponential Laplacian operator $e^{(c_i-c_j)\Delta t\mathcal{L}}$ and the conditional expectation operator $\tilde{\mathbb{E}}_{c_i,c_j,\Delta t}$?

By answering the above question, we can also reveal the relationship between the time semidiscrete SRK and IFRK schemes. To answer the question, we analyze the eigenvalues of the two operators under the periodic boundary condition. Let $\boldsymbol{k} = (k_1,\ldots,k_d)$ with $k_l \in \mathbb{Z}$ for $1 \le l \le d$. By using the definition of $\mathcal{L}$, it is easy to get the $\boldsymbol{k}$-th eigenvalue of $e^{(c_i-c_j)\Delta t\mathcal{L}}$ as

$$
\lambda_{\boldsymbol{k}}^e = e^{-(c_i-c_j)\Delta t\frac{2\pi^2}{a^2}\sum\limits_{l=1}^{d}\sigma_l^2 k_l^2}.
$$

Now we derive the $\boldsymbol{k}$-th eigenvalue of $\tilde{\mathbb{E}}_{c_i,c_j,\Delta t}$. By using the fact that

$$X_{t_n^j}^{t_n^i,\boldsymbol{x}} = \boldsymbol{x} + \sigma\big(W_{t_n^j} - W_{t_n^i}\big)$$

and $W_t = (W_t^1,\ldots,W_t^d)^\top$ with $W_t^l \overset{iid}{\sim} N(0,t)$, we deduce

$$\begin{aligned}\tilde{\mathbb{E}}_{c_i,c_j,\Delta t}\left[e^{\mathrm{i}\frac{2\pi}{a}\boldsymbol{x}\cdot\boldsymbol{k}}\right] &= \mathbb{E}\left[e^{\mathrm{i}\frac{2\pi}{a}(\boldsymbol{x}+\sigma(W_{t_n^j}-W_{t_n^i}))\cdot\boldsymbol{k}}\right] \\ &= e^{\mathrm{i}\frac{2\pi}{a}\boldsymbol{x}\cdot\boldsymbol{k}}\prod_{l=1}^{d}\mathbb{E}\left[e^{\mathrm{i}\frac{2\pi}{a}\sigma_l(W_{t_n^j}^l-W_{t_n^i}^l)k_l}\right] \\ &= e^{\mathrm{i}\frac{2\pi}{a}\boldsymbol{x}\cdot\boldsymbol{k}}e^{-(c_i-c_j)\Delta t\frac{2\pi^2}{a^2}\sum\limits_{l=1}^{d}\sigma_l^2k_l^2},\end{aligned}$$

which indicates that the $\boldsymbol{k}$-th eigenvalue of $\tilde{\mathbb{E}}_{c_i,c_j,\Delta t}$ is

$$\lambda_{\boldsymbol{k}}^{\mathbb{E}} = e^{-(c_i-c_j)\Delta t\frac{2\pi^2}{a^2}\sum\limits_{l=1}^{d}\sigma_l^2k_l^2}.$$

Since $\lambda_{\boldsymbol{k}}^{e} = \lambda_{\boldsymbol{k}}^{\mathbb{E}}$, the operators $e^{(c_i-c_j)\Delta t\mathcal{L}}$ and $\tilde{\mathbb{E}}_{c_i,c_j,\Delta t}$ have the same eigenvalues. Therefore, we conclude that they are two different representations for the same one linear operator, which answers the above question. Moreover, this answer to the above question reveals that the time semidiscrete SRK and IFRK schemes are essentially equivalent.

Nevertheless, the discretizations for the two different operators will lead to totally different fully discrete SRK and IFRK schemes as shown in the next section. The main reason is that $e^{(c_i-c_j)\Delta t\mathcal{L}}$ is a differential operator while $\tilde{\mathbb{E}}_{c_i,c_j,\Delta t}$ is an integral operator, and thus the discretizations for them are carried out in totally different ways.

4 The fully discrete SRK schemes

In this section, to construct the fully discrete SRK schemes, we adopt the Sinc quadrature rule to approximate the expectations in the time semidiscrete scheme (3.8). To this end, we introduce the following uniform mesh D_h of the domain $D = (0,a)^d$ as

$$D_h = \{\boldsymbol{x_k} = \boldsymbol{k}\Delta x, 1 \le k_i \le N_x, i = 1,\ldots,d\},$$

where $\boldsymbol{k} = (k_1,\ldots,k_d)^\top$ is a multi-index and $\Delta x = a/N_x$ is the uniform mesh size with N_x being an even integer.

4.1 Sinc approximations

In this subsection, we recall some basic ideas of the Sinc approximations [25,34].

First, we define the Sinc function on the real line $\mathbb{R}$ by

$$\operatorname{sinc}(x)=\begin{cases}\dfrac{\sin(\pi x)}{\pi x}, & x\neq 0,\\ 1, & x=0.\end{cases}$$

Moreover, we let $B(h)$ denote the class of entire functions g such that on the real line $\mathbb{R}, g\in L^2(\mathbb{R})$, while in the entire complex plane $\mathbb{C}, g$ is of the following exponential type:

$$|g(z)|\leq K\exp\left(\frac{\pi|z|}{h}\right),\quad \forall z\in\mathbb{C},$$

where K and h are positive constants. Then for the functions in $B(h)$, we have the following series convergence results [25].

Theorem 4.1. *If $g\in B(h)$, then for all $z\in\mathbb{C}$, we have*

$$g(z)=\sum_{k=-\infty}^{\infty} g(kh)\operatorname{sinc}\left(\frac{z-kh}{h}\right).$$

Moreover, if $\sum\limits_{k=-\infty}^{\infty} g(kh)$ converges, then for sufficiently small h, it holds that

$$\int_{\mathbb{R}} g(x)dx=h\sum_{k=-\infty}^{\infty} g(kh).$$

The above theorem indicates that we can define the following truncated Sinc approximation for $\int_{\mathbb{R}} g(x)dx$ as

$$T_M(g,h)=h\sum_{k=-M}^{M} g(kh). \tag{4.1}$$

Definition 4.1. *We call $T_M(g,h)$ defined in* (4.1) *the Sinc quadrature rule for the integral $\int_{\mathbb{R}} g(x)dx$ and let $\eta_M(g,h)$ be the truncation error of $T_M(g,h)$, that is,*

$$\eta_M(g,h)=\int_{\mathbb{R}} g(x)dx-T_M(g,h).$$

For the estimate of $\eta_M(g,h)$, we have the following theorem [38].

Theorem 4.2. *Assume that g is bounded. Then for sufficiently small h, if there exists a positive number γ_0 such that $\gamma_0\leq Mh^2$, it holds that*

$$|\eta_M(g,h)|\leq C_{\gamma_0,g}h\exp\left(-\frac{M^2h^2}{2}\right),$$

where $C_{\gamma_0,g}$ is a positive constant depending only on γ_0 and $\|g\|_{L^\infty}$.

4.2 The fully discrete schemes

To construct the fully discrete schemes, we use the Sinc quadrature rule to approximate the expectations in the time semidiscrete scheme (3.8). For simplicity of presentation, we assume that

$$\sigma_i = \sigma_0, \quad i = 1,\ldots,d$$

for a given positive constant σ_0. To proceed, we let $v:\mathbb{R}^d \to \mathbb{R}$ be some smooth function and write the expectations in (3.8) in the general form

$$\mathbb{E}\left[v\left(X_r^{t,\boldsymbol{x}}\right)\right], \quad 0 \le t \le r \le T,$$

where

$$X_r^{t,\boldsymbol{x}} = \boldsymbol{x} + \sigma_0 (W_r - W_t).$$

For the case $r = t$, we get $X_t^{t,\boldsymbol{x}} = \boldsymbol{x}$ and thus

$$\mathbb{E}\left[v\left(X_t^{t,\boldsymbol{x}}\right)\right] = \mathbb{E}[v(\boldsymbol{x})] = v(\boldsymbol{x}). \tag{4.2}$$

For the case $r > t$, since $W_t = (W_t^1,\ldots,W_t^d)^\top$ with $W_t^l \overset{iid}{\sim} N(0,t)$, by combining with the Sinc quadrature rule, we deduce

$$\begin{aligned}
\mathbb{E}\left[v\left(X_r^{t,\boldsymbol{x}}\right)\right] &= \mathbb{E}\left[v\left(\boldsymbol{x} + \sigma_0 (W_r - W_t)\right)\right] \\
&= \int_{\mathbb{R}^d} v\left(\boldsymbol{x} + \sigma_0 \sqrt{r-t}\,\boldsymbol{p}\right) \left(\frac{1}{\sqrt{2\pi}}\right)^d \exp\left(-\frac{\boldsymbol{p}^\top \boldsymbol{p}}{2}\right) d\boldsymbol{p} \\
&= \sum_{\boldsymbol{k}=-M}^{M} v\left(\boldsymbol{x} + \sigma_0 \sqrt{r-t}\,h\boldsymbol{k}\right) \boldsymbol{\alpha}_{\boldsymbol{k}} + R_E^M(\boldsymbol{x}) \\
&= \sum_{\boldsymbol{k}=-M}^{M} v\left(\boldsymbol{x} + \sigma_0 \sqrt{r-t}\,h\boldsymbol{k}\right) \boldsymbol{\beta}_{\boldsymbol{k}}^M + \tilde{R}_E^M(\boldsymbol{x}),
\end{aligned} \tag{4.3}$$

where

$$\boldsymbol{k} = (k_1,\ldots,k_d)^\top, \quad \boldsymbol{\alpha}_{\boldsymbol{k}} = \prod_{i=1}^{d} \alpha_{k_i}, \quad \alpha_{k_i} = \frac{h}{\sqrt{2\pi}} \exp\left(-\frac{k_i^2 h^2}{2}\right),$$

and

$$\sum_{\boldsymbol{k}=-M}^{M} = \sum_{k_1=-M}^{M} \cdots \sum_{k_d=-M}^{M}, \quad \boldsymbol{\beta}_{\boldsymbol{k}}^M = \frac{\boldsymbol{\alpha}_{\boldsymbol{k}}}{\sum_{\boldsymbol{k}=-M}^{M} \boldsymbol{\alpha}_{\boldsymbol{k}}}. \tag{4.4}$$

Here $R_E^M(\boldsymbol{x})$ and $\tilde{R}_E^M(\boldsymbol{x})$ are the Sinc truncation errors defined as

$$\begin{aligned}
R_E^M(\boldsymbol{x}) = &\int_{\mathbb{R}^d} v\left(\boldsymbol{x} + \sigma_0 \sqrt{r-t}\,\boldsymbol{p}\right) \left(\frac{1}{\sqrt{2\pi}}\right)^d \exp\left(-\frac{\boldsymbol{p}^\top \boldsymbol{p}}{2}\right) d\boldsymbol{p} \\
&- \sum_{\boldsymbol{k}=-M}^{M} v\left(\boldsymbol{x} + \sigma_0 \sqrt{r-t}\,h\boldsymbol{k}\right) \boldsymbol{\alpha}_{\boldsymbol{k}},
\end{aligned} \tag{4.5a}$$

$$\begin{aligned}\tilde{R}_E^M(\boldsymbol{x}) = &\int_{\mathbb{R}^d} v\big(\boldsymbol{x}+\sigma_0\sqrt{r-t}\boldsymbol{p}\big)\left(\frac{1}{\sqrt{2\pi}}\right)^d \exp\left(-\frac{\boldsymbol{p}^\top\boldsymbol{p}}{2}\right)d\boldsymbol{p}\\ &-\sum_{\boldsymbol{k}=-M}^{M} v\big(\boldsymbol{x}+\sigma_0\sqrt{r-t}h\boldsymbol{k}\big)\boldsymbol{\beta}_{\boldsymbol{k}}^M.\end{aligned} \tag{4.5b}$$

Take $\boldsymbol{x}=\boldsymbol{x_m}\in D_h$ in (4.3) and choose the free parameter h by

$$\sigma_0\sqrt{r-t}h=\Delta x, \tag{4.6}$$

so that the points

$$\boldsymbol{x_m}+\sigma_0\sqrt{r-t}h\boldsymbol{k}=\boldsymbol{x_m}+\boldsymbol{k}\Delta x=\boldsymbol{x_{m+k}}\in D_h. \tag{4.7}$$

Thus, we define the approximation of $\mathbb{E}[v(X_r^{t,\boldsymbol{x_m}})]$ as

$$\mathbb{E}_M\big[v\big(X_r^{t,\boldsymbol{x_m}}\big)\big]=\sum_{\boldsymbol{k}=-M}^{M} v(\boldsymbol{x_{m+k}})\boldsymbol{\beta}_{\boldsymbol{k}}^M,\quad \boldsymbol{x_m}\in D_h. \tag{4.8}$$

To write the equations in (4.8) in matrix form, we define the matrix $G_M(r-t)$ of order N_x as

$$G_M(r-t)=\frac{1}{\sum\limits_{k=-M}^{M}\alpha_k}\begin{pmatrix} \alpha_0 & \alpha_1 & \cdots & \alpha_M & \cdots & \alpha_{-M} & \cdots & \cdots & \alpha_{-2} & \alpha_{-1}\\ \alpha_{-1} & \alpha_0 & \alpha_1 & \cdots & \alpha_M & \cdots & \alpha_{-M} & \cdots & \alpha_{-3} & \alpha_{-2}\\ \vdots & \vdots & \vdots & & \vdots & & \vdots & \vdots & \vdots & \vdots\\ \alpha_2 & \alpha_3 & \cdots & \alpha_M & \cdots & \alpha_{-M} & \cdots & \alpha_{-1} & \alpha_0 & \alpha_1\\ \alpha_1 & \alpha_2 & \cdots & \cdots & \alpha_M & \cdots & \alpha_{-M} & \cdots & \alpha_{-1} & \alpha_0 \end{pmatrix},$$

where

$$\alpha_k=\frac{h}{\sqrt{2\pi}}\exp\left(-\frac{k^2h^2}{2}\right),\quad h=\frac{\Delta x}{\sigma_0\sqrt{r-t}},$$

that is,

$$\alpha_k=\frac{\Delta x}{\sigma_0\sqrt{2\pi(r-t)}}\exp\left(-\frac{k^2\Delta x^2}{2\sigma_0^2(r-t)}\right).$$

Let $\boldsymbol{v}$ and $\boldsymbol{V}$ be the vectors of $\{v(\boldsymbol{x_m})\}$ and $\{\mathbb{E}_M[v(X_r^{t,\boldsymbol{x_m}})]\}$ ordered lexicographically, respectively, then we can write the Eq. (4.8) as

$$\boldsymbol{V}=G(r-t)\boldsymbol{v}, \tag{4.9}$$

where the matrix $G(r-t)$ is defined by

$$G(r-t)=\begin{cases} G_M(r-t), & d=1,\\ G_M(r-t)\otimes G_M(r-t), & d=2,\\ G_M(r-t)\otimes G_M(r-t)\otimes G_M(r-t), & d=3.\end{cases} \tag{4.10}$$

Let $\boldsymbol{u}_n$ (or $\boldsymbol{u}_n^{(i)}$) $\in \mathbb{R}^{N_x^d}$ be the approximations of the solution $u(t_n,\boldsymbol{x})$ (or $u(t_n^i,\boldsymbol{x})$) at the spatial points in D_h, which are ordered lexicographically. Then by using (4.9) to approximate the expectations in the semidiscrete scheme (3.8), we get the following fully discrete s-stage SRK scheme in the matrix form:

$$\begin{aligned} &\boldsymbol{u}_n^{(0)} = \boldsymbol{u}_{n+1}, \\ &\boldsymbol{u}_n^{(i)} = \sum_{j=0}^{i-1} G\big(t_n^j - t_n^i\big)\big(\alpha_{ij}\boldsymbol{u}_n^{(j)} + \Delta t \beta_{ij} f\big(\boldsymbol{u}_n^{(j)}\big)\big), \quad i=1,\dots,s, \\ &\boldsymbol{u}_n = \boldsymbol{u}_n^{(s)}, \end{aligned} \tag{4.11}$$

where $G(t_n^j - t_n^i)$ is defined by (4.10) with the free parameter $h = h_{ij}$ given by

$$h_{ij} = \frac{\Delta x}{\sigma_0 \sqrt{t_n^j - t_n^i}}. \tag{4.12}$$

It is worth noting that for $t_n^i = t_n^j$, the matrix $G(0)$ becomes the unit matrix of order N_x^d, which can also be obtained from the equality in (4.2).

Remark 4.1. When the elements of σ in (1.1) are not a constant, we can also define the matrix $G(r-t)$ by taking different free parameters in different dimensions. Specifically, in the l-th dimension, we choose the free parameter h_l by

$$h_l = \frac{\Delta x}{\sigma_l \sqrt{r-t}}, \quad l=1,\dots,d.$$

Remark 4.2. Except its spectral accuracy, the main reason we choose the Sinc quadrature rule over other quadrature rules is that its quadrature points are uniform and contain a free parameter h. Thus, by setting different values of h for different time increments between different intermediate times, we can obtain different uniform quadrature points to avoid using the interpolation when approximating the conditional expectations in high-order time semidiscrete SRK methods with multi-stages.

4.3 The fully discrete MBP

In this subsection, we show the MBP-preserving of the fully discrete SRK scheme. To this end, we denote by $\|\cdot\|_\infty$ the vector or matrix maximum norm. Then by (4.10), we have

$$\|G(r-t)\|_\infty = \max_i \sum_{j=1}^{N_x^d} \big(G(r-t)\big)_{ij} = 1, \quad \forall\, 0 \le t \le r \le T. \tag{4.13}$$

Let r_0^+ and r_0^- be the two parameters defined in (3.9) and (3.10). Then we have the following theorem.

Theorem 4.3. *Assume that f satisfies the conditions* (3.9) *and* (3.10)*, then if $\|\boldsymbol{u}_{n+1}\|_\infty \le \rho$, the solution $\boldsymbol{u}_n$ obtained from* (4.11) *satisfies $\|\boldsymbol{u}_n\|_\infty \le \rho$, provided that*

$$\Delta t \le \mathcal{C} r_0^+, \quad \mathcal{C} = \min_{i,j} \frac{\alpha_{ij}}{\beta_{ij}}, \tag{4.14}$$

when β_{ij} are all nonnegative, or satisfies

$$\Delta t \le \mathcal{C} \min\{r_0^+, r_0^-\}, \quad \mathcal{C} = \min_{i,j} \frac{\alpha_{ij}}{|\beta_{ij}|}, \tag{4.15}$$

whenever there is a negative β_{ij}.

Proof. Since $\|\boldsymbol{u}_{n+1}\|_\infty \le \rho$, we can suppose that $\|\boldsymbol{u}_{n+1}^{(j)}\|_\infty \le \rho$ for all $j \le i-1$. For the i-th stage, by using (4.13) and the conditions in the theorem, we deduce

$$\begin{aligned}
\|\boldsymbol{u}_n^{(i)}\|_\infty &\le \sum_{j=0}^{i-1} \left\| G\left(t_n^j - t_n^i\right) \right\|_\infty \left\| \alpha_{ij} \boldsymbol{u}_n^{(j)} + \Delta t \beta_{ij} f\left(\boldsymbol{u}_n^{(j)}\right) \right\|_\infty \\
&\le \sum_{j=0}^{i-1} \alpha_{ij} \left\| \boldsymbol{u}_n^{(j)} + \Delta t \frac{\beta_{ij}}{\alpha_{ij}} f\left(\boldsymbol{u}_n^{(j)}\right) \right\|_\infty \\
&\le \sum_{j=0}^{i-1} \alpha_{ij} \rho = \rho.
\end{aligned}$$

Then by induction, we get $\|\boldsymbol{u}_n\|_\infty \le \rho$, which completes the proof. □

Now we present some specific fully discrete MBP-preserving SRK schemes with up to fourth-order accuracy as below.

- The one-stage first-order SRK (SRK1) scheme,

$$\boldsymbol{u}_n = G(\Delta t)\big(\boldsymbol{u}_{n+1} + \Delta t f(\boldsymbol{u}_{n+1})\big). \tag{4.16}$$

- The two-stage second-order SRK (SRK2) scheme,

$$\begin{aligned}
\boldsymbol{u}_n^{(1)} &= G(\Delta t)\big(\boldsymbol{u}_{n+1} + \Delta t f(\boldsymbol{u}_{n+1})\big), \\
\boldsymbol{u}_n &= \frac{1}{2} G(\Delta t) \boldsymbol{u}_{n+1} + \frac{1}{2}\big(\boldsymbol{u}_n^{(1)} + \Delta t f\big(\boldsymbol{u}_n^{(1)}\big)\big).
\end{aligned} \tag{4.17}$$

- The three-stage third-order SRK (SRK3) scheme,

$$\boldsymbol{u}_n^{(1)} = G\left(\frac{2\Delta t}{3}\right)\left(\boldsymbol{u}_{n+1} + \frac{2\Delta t}{3} f(\boldsymbol{u}_{n+1})\right), \tag{4.18a}$$

$$\boldsymbol{u}_n^{(2)} = \frac{2}{3} G\left(\frac{2\Delta t}{3}\right) \boldsymbol{u}_{n+1} + \frac{1}{3}\left(\boldsymbol{u}_n^{(1)} + \frac{4\Delta t}{3} f\big(\boldsymbol{u}_n^{(1)}\big)\right), \tag{4.18b}$$

$$\begin{aligned}\boldsymbol{u}_n=&\frac{59}{128}G(\Delta t)\boldsymbol{u}_{n+1}+\frac{15}{128}G(\Delta t)\left(\boldsymbol{u}_{n+1}+\frac{4\Delta t}{3}f(\boldsymbol{u}_{n+1})\right)\\&+\frac{27}{64}G\left(\frac{\Delta t}{3}\right)\left(\boldsymbol{u}_n^{(2)}+\frac{4\Delta t}{3}f\big(\boldsymbol{u}_n^{(2)}\big)\right).\end{aligned}\tag{4.18c}$$

- The four-stage fourth-order SRK (SRK4) scheme,

$$\left\{\begin{aligned}\boldsymbol{u}_n^{(1)}=&\left(\frac{\Delta t}{2}\right)\left(\boldsymbol{u}_{n+1}+\frac{\Delta t}{2}f(\boldsymbol{u}_{n+1})\right),\\ \boldsymbol{u}_n^{(2)}=&\frac{1}{2}G\left(\frac{\Delta t}{2}\right)\left(\boldsymbol{u}_{n+1}-\frac{\Delta t}{2}f(\boldsymbol{u}_{n+1})\right)+\frac{1}{2}\big(\boldsymbol{u}_n^{(1)}+\Delta tf\big(\boldsymbol{u}_n^{(1)}\big)\big),\\ \boldsymbol{u}_n^{(3)}=&\frac{1}{9}G(\Delta t)\big(\boldsymbol{u}_{n+1}-\Delta tf(\boldsymbol{u}_{n+1})\big)+\frac{2}{9}G\left(\frac{\Delta t}{2}\right)\left(\boldsymbol{u}_n^{(1)}-\frac{3\Delta t}{2}f\big(\boldsymbol{u}_n^{(1)}\big)\right)\\&+\frac{2}{3}G\left(\frac{\Delta t}{2}\right)\left(\boldsymbol{u}_n^{(2)}+\frac{3\Delta t}{2}f\big(\boldsymbol{u}_n^{(2)}\big)\right),\\ \boldsymbol{u}_n=&\frac{1}{3}G\left(\frac{\Delta t}{2}\right)\left(\boldsymbol{u}_n^{(1)}+\frac{\Delta t}{2}f\big(\boldsymbol{u}_n^{(1)}\big)\right)+\frac{1}{3}G\left(\frac{\Delta t}{2}\right)\boldsymbol{u}_n^{(2)}\\&+\frac{1}{3}\left(\boldsymbol{u}_n^{(3)}+\frac{\Delta t}{2}f\big(\boldsymbol{u}_n^{(3)}\big)\right).\end{aligned}\right.\tag{4.19}$$

We also list the values of $\mathcal{C}$ in Theorem 4.3 for the schemes (4.16)-(4.19) as

$$\mathcal{C}=\left(1,1,\frac{3}{4},\frac{2}{3}\right).$$

It is reasonable to assert that the schemes (4.16)-(4.19) are optimal MBP-preserving SRK schemes from the point of the value of $\mathcal{C}$. To illustrate this point, we give some other three-stage third-order and four-stage fourth-order MBP-preserving SRK schemes as below.

- The three-stage third-order SRK (SRK3-I) scheme,

$$\left\{\begin{aligned}\boldsymbol{u}_n^{(1)}=&G\left(\frac{\Delta t}{3}\right)\left(\boldsymbol{u}_{n+1}+\frac{\Delta t}{3}f(\boldsymbol{u}_{n+1})\right),\\ \boldsymbol{u}_n^{(2)}=&\frac{1}{3}G\left(\frac{2\Delta t}{3}\right)\left(\boldsymbol{u}_{n+1}-\frac{2\Delta t}{3}f(\boldsymbol{u}_{n+1})\right)+\frac{2}{3}G\left(\frac{\Delta t}{3}\right)\big(\boldsymbol{u}_n^{(1)}+\Delta tf\big(\boldsymbol{u}_n^{(1)}\big)\big),\\ \boldsymbol{u}_{n+1}=&\frac{3}{4}G\left(\frac{2\Delta t}{3}\right)\left(\boldsymbol{u}_n^{(1)}-\frac{2\Delta t}{9}f\big(\boldsymbol{u}_n^{(1)}\big)\right)+\frac{1}{4}G\left(\frac{\Delta t}{3}\right)\big(\boldsymbol{u}_n^{(2)}+3\Delta tf\big(\boldsymbol{u}_n^{(2)}\big)\big).\end{aligned}\right.\tag{4.20}$$

- The four-stage fourth-order SRK (SRK4-I) scheme,

$$\boldsymbol{u}_n^{(1)}=G\left(\frac{\Delta t}{2}\right)\left(\boldsymbol{u}_{n+1}+\frac{\Delta t}{2}f(\boldsymbol{u}_{n+1})\right),\tag{4.21a}$$

$$\boldsymbol{u}_n^{(2)} = \frac{1}{2} G\left(\frac{\Delta t}{2}\right)\left(\boldsymbol{u}_{n+1} - \frac{\Delta t}{2} f(\boldsymbol{u}_{n+1})\right) + \frac{1}{2}\left(\boldsymbol{u}_n^{(1)} + \Delta t f\left(\boldsymbol{u}_n^{(1)}\right)\right), \tag{4.21b}$$

$$\begin{aligned}\boldsymbol{u}_n^{(3)} = &\frac{1}{4} G(\Delta t)\left(\boldsymbol{u}_{n+1} - \frac{\Delta t}{2} f(\boldsymbol{u}_{n+1})\right) + \frac{1}{4} G\left(\frac{\Delta t}{2}\right)\left(\boldsymbol{u}_n^{(1)} - \Delta t f\left(\boldsymbol{u}_n^{(1)}\right)\right) \\ &+ \frac{1}{2} G\left(\frac{\Delta t}{2}\right)\left(\boldsymbol{u}_n^{(2)} + 2\Delta t f\left(\boldsymbol{u}_n^{(2)}\right)\right),\end{aligned} \tag{4.21c}$$

$$\begin{aligned}\boldsymbol{u}_{n+1} = &\frac{1}{3} G\left(\frac{\Delta t}{2}\right)\left(\boldsymbol{u}_n^{(1)} + \frac{\Delta t}{2} f\left(\boldsymbol{u}_n^{(1)}\right)\right) + \frac{1}{3} G\left(\frac{\Delta t}{2}\right)\boldsymbol{u}_n^{(2)} \\ &+ \frac{1}{3}\left(\boldsymbol{u}_n^{(3)} + \frac{\Delta t}{2} f\left(\boldsymbol{u}_n^{(3)}\right)\right).\end{aligned} \tag{4.21d}$$

Then we obtain the values of $\mathcal{C}$ for the schemes (4.20) and (4.21) as

$$\mathcal{C} = \left(\frac{1}{3}, \frac{1}{2}\right),$$

which indicates that the schemes (4.18) and (4.19) are indeed more optimal third-order and fourth-order MBP-preserving SRK schemes, respectively.

4.4 The fully discrete error estimate

In this subsection, we derive the error estimate of the fully discrete SRK scheme. To this end, we introduce the following two useful lemmas.

Lemma 4.1. *For sufficiently small h, if there exists a positive number γ_0 such that $\gamma_0 \le Mh^2$, it holds that*

$$\left|\sum_{\boldsymbol{k}=-M}^{M} \boldsymbol{\alpha}_{\boldsymbol{k}} - 1\right| \le Ch\exp\left(-\frac{M^2h^2}{2}\right),$$

where C is a positive constant depending only on γ_0.

Proof. By repeatedly applying Theorem 4.2, we get

$$\left|\int_{\mathbb{R}^d} \exp\left(-\frac{\boldsymbol{x}^\top \boldsymbol{x}}{2}\right) d\boldsymbol{x} - h^d \sum_{\boldsymbol{k}=-M}^{M} \exp\left(-\frac{h^2 \boldsymbol{k}^\top \boldsymbol{k}}{2}\right)\right| \le Ch\exp\left(-\frac{M^2h^2}{2}\right).$$

Then by using the definition of $\boldsymbol{\alpha}_{\boldsymbol{k}}$ in (4.4), we deduce

$$\left|\left(\sqrt{2\pi}\right)^d - \left(\sqrt{2\pi}\right)^d \sum_{\boldsymbol{k}=-M}^{M} \boldsymbol{\alpha}_{\boldsymbol{k}}\right| \le Ch\exp\left(-\frac{M^2h^2}{2}\right),$$

which completes the proof. □

Lemma 4.2. *Assume that v is bounded. For sufficiently small h, if there exists a positive number γ_0 such that $\gamma_0 \le Mh^2$, it holds that*

$$\|\tilde{R}_E^M\|_\infty \le Ch\exp\left(-\frac{M^2h^2}{2}\right),$$

where C is a positive constant depending only on γ_0 and $\|v\|_{L^\infty}$.

Proof. By using the definitions of $\boldsymbol{\beta}_{\boldsymbol{k}}^M, R_E^M(\boldsymbol{x})$ and $\tilde{R}_E^M(\boldsymbol{x})$ in (4.4)-(4.5), we get

$$\begin{aligned}
|\tilde{R}_E^M(\boldsymbol{x})| &= \left|\mathbb{E}\left[v\left(X_r^{t,\boldsymbol{x}}\right)\right] - \sum_{\boldsymbol{k}=-M}^{M} v\left(\boldsymbol{x}+\sigma\sqrt{r-t}h\boldsymbol{k}\right)\boldsymbol{\beta}_{\boldsymbol{k}}^M\right| \\
&= \left|R_E^M(\boldsymbol{x}) + \sum_{\boldsymbol{k}=-M}^{M} \boldsymbol{\alpha}_{\boldsymbol{k}}\left(1-\frac{1}{\sum_{\boldsymbol{k}=-M}^{M}\boldsymbol{\alpha}_{\boldsymbol{k}}}\right) v\left(\boldsymbol{x}+\sigma\sqrt{r-t}h\boldsymbol{k}\right)\right| \\
&\le \|R_E^M\|_{L^\infty} + \left|1-\frac{1}{\sum_{\boldsymbol{k}=-M}^{M}\boldsymbol{\alpha}_{\boldsymbol{k}}}\right| \sum_{\boldsymbol{k}=-M}^{M} \boldsymbol{\alpha}_{\boldsymbol{k}} \|v\|_{L^\infty} \\
&= \|R_E^M\|_{L^\infty} + \left|\sum_{\boldsymbol{k}=-M}^{M}\boldsymbol{\alpha}_{\boldsymbol{k}} - 1\right| \|v\|_{L^\infty}.
\end{aligned}$$

Since v is bounded, Theorem 4.2 and Lemma 4.1 imply that

$$\begin{aligned}
&\|R_E^M\|_{L^\infty} \le Ch\exp\left(-\frac{M^2h^2}{2}\right), \\
&\left|\sum_{\boldsymbol{k}=-M}^{M}\boldsymbol{\alpha}_{\boldsymbol{k}} - 1\right| \|v\|_{L^\infty} \le Ch\exp\left(-\frac{M^2h^2}{2}\right),
\end{aligned}$$

which completes the proof. ☐

Now we turn to the error analysis of the fully discrete SRK scheme. To proceed, we write (4.11) in the following Butcher form:

$$\begin{aligned}
&\boldsymbol{u}_n^{(0)} = \boldsymbol{u}_{n+1}, \\
&\boldsymbol{u}_n^{(i)} = G\left(t_{n+1}-t_n^i\right)\boldsymbol{u}_{n+1} + \Delta t\sum_{j=0}^{i-1} a_{ij} G\left(t_n^j - t_n^i\right) f\left(\boldsymbol{u}_n^{(j)}\right), \quad i=1,\ldots,s, \\
&\boldsymbol{u}_n = \boldsymbol{u}_n^{(s)}.
\end{aligned} \tag{4.22}$$

Let $\boldsymbol{U}_n$ and $\boldsymbol{U}_n^{(i)}$ be the restrictions of $u_n(\boldsymbol{x})$ and $u_n^{(i)}(\boldsymbol{x})$ on the mesh D_h, respectively, and then we have

$$\begin{aligned}
&\boldsymbol{U}_n^{(0)} = \boldsymbol{U}_{n+1}, \\
&\boldsymbol{U}_n^{(i)} = G\left(t_{n+1}-t_n^i\right)\boldsymbol{U}_{n+1} + \Delta t\sum_{j=0}^{i-1} a_{ij} G\left(t_n^j - t_n^i\right) f\left(\boldsymbol{U}_n^{(j)}\right) + \boldsymbol{r}_n^{(i)}, \quad i=1,\ldots,s, \\
&\boldsymbol{U}_n = \boldsymbol{U}_n^{(s)},
\end{aligned} \tag{4.23}$$

where $\{\boldsymbol{r}_n^{(i)}\}$ are the corresponding Sinc truncation errors. Define the constant h_0 as

$$h_0 = \frac{\Delta x}{\sigma_0 \sqrt{\Delta t}}, \tag{4.24}$$

then the free parameter h_{ij} defined in (4.12) for $G(t_n^j - t_n^i)$ satisfies

$$h_{ij} = \frac{\Delta x}{\sigma_0 \sqrt{t_n^j - t_n^i}} \geq \frac{\Delta x}{\sigma_0 \sqrt{\Delta t}} = h_0. \tag{4.25}$$

Theorem 4.4. *Let $u_n(\boldsymbol{x})$ and $\boldsymbol{u}_n$ be the numerical solutions obtained from the time semidiscrete SRK scheme* (3.8) *with $u_{N_t}(\boldsymbol{x}) = \varphi(\boldsymbol{x})$ and the fully discrete SRK scheme* (4.22) *with $\boldsymbol{u}_{N_t} = \boldsymbol{U}_{N_t}$, respectively. Assume that $\|\varphi\|_{L^\infty} \leq \rho$, $Mh_0 > 1$ and $\{h_{ij}\}$ are sufficiently small. Then under the conditions in Theorem* 3.1, *we have*

$$\|\boldsymbol{U}_n - \boldsymbol{u}_n\|_\infty \leq \frac{C_2 h_0}{\Delta t} e^{-\frac{M^2 h_0^2}{2}} \left(e^{\tilde{C} s (T - t_n)} - 1 \right), \tag{4.26}$$

where $\tilde{C} = \max_{|\xi| \leq \rho} |f'(\xi)|$ and the positive constant C_2 is independent of Δt and h_0.

Proof. Define the spatial errors of the scheme (4.22) as

$$\boldsymbol{e}_n = \boldsymbol{U}_n - \boldsymbol{u}_n, \quad \boldsymbol{e}_n^{(i)} = \boldsymbol{U}_n^{(i)} - \boldsymbol{u}_n^{(i)}, \quad i = 0, \ldots, s.$$

By combining (4.22) and (4.23), we get for $i = 1, \ldots, s$,

$$\boldsymbol{e}_n^{(i)} = G\left(t_{n+1} - t_n^i\right) \boldsymbol{e}_{n+1} + \Delta t \sum_{j=0}^{i-1} a_{ij} G\left(t_n^j - t_n^i\right) \left(f\left(\boldsymbol{U}_n^{(j)}\right) - f\left(\boldsymbol{u}_n^{(j)}\right) \right) + \boldsymbol{r}_n^{(i)}.$$

Based on the conditions in the theorem, using Theorems 3.1 and 4.3, we have

$$\left\|\boldsymbol{U}_n^{(i)}\right\|_\infty \leq \rho, \quad \left\|\boldsymbol{u}_n^{(i)}\right\|_\infty \leq \rho, \quad i = 0, \ldots, s,$$

which leads to

$$\begin{aligned} \left\|\boldsymbol{e}_n^{(i)}\right\|_\infty &\leq \|\boldsymbol{e}_{n+1}\|_\infty + \Delta t \sum_{j=0}^{i-1} \left\|G\left(t_n^j - t_n^i\right)\right\|_\infty \left\|f\left(\boldsymbol{U}_n^{(j)}\right) - f\left(\boldsymbol{u}_n^{(j)}\right)\right\|_\infty + \left\|\boldsymbol{r}_n^{(i)}\right\|_\infty \\ &\leq \|\boldsymbol{e}_{n+1}\|_\infty + \tilde{C} \Delta t \sum_{j=0}^{i-1} \left\|\boldsymbol{e}_n^{(j)}\right\|_\infty + \left\|\boldsymbol{r}_n^{(i)}\right\|_\infty, \quad i = 1, \ldots, s. \end{aligned} \tag{4.27}$$

When $Mh_0 > 1$, it is easy to verify that $he^{-M^2 h^2/2}$ is decreasing with respect to h for $h \geq h_0$. Since $h_{ij} \geq h_0$ as shown in (4.25), using Lemma 4.2, we obtain

$$\left\|\boldsymbol{r}_n^{(i)}\right\|_\infty \leq \sum_{j=0}^{i-1} C h_{ij} e^{-\frac{M^2 h_{ij}^2}{2}} \leq C s h_0 e^{-\frac{M^2 h_0^2}{2}}. \tag{4.28}$$

Inserting (4.28) into (4.27) yields

$$\|\boldsymbol{e}_n^{(i)}\|_\infty \leq \|\boldsymbol{e}_{n+1}\|_\infty + \tilde{C}\Delta t \sum_{j=0}^{i-1} \|\boldsymbol{e}_n^{(j)}\|_\infty + Csh_0 e^{-\frac{M^2h_0^2}{2}}.$$

We claim that

$$\|\boldsymbol{e}_n^{(j)}\|_\infty \leq (1+\tilde{C}\Delta t)^j \left(\|\boldsymbol{e}_{n+1}\|_\infty + Csh_0 e^{-\frac{M^2h_0^2}{2}}\right), \quad j=0,\ldots,s. \tag{4.29}$$

Indeed, we assume that (4.29) holds for $j=0,\ldots,i-1$. Then by induction, we get

$$\begin{aligned}\|\boldsymbol{e}_n^{(i)}\|_\infty &\leq \left(1+\tilde{C}\Delta t \sum_{j=0}^{i-1}(1+\tilde{C}\Delta t)^j\right)\left(\|\boldsymbol{e}_{n+1}\|_\infty + Csh_0 e^{-\frac{M^2h_0^2}{2}}\right) \\ &= (1+\tilde{C}\Delta t)^i \left(\|\boldsymbol{e}_{n+1}\|_\infty + Csh_0 e^{-\frac{M^2h_0^2}{2}}\right), \quad i=0,\ldots,s.\end{aligned}$$

Since $\boldsymbol{e}_n = \boldsymbol{e}_n^{(s)}$, we have

$$\begin{aligned}\|\boldsymbol{e}_n\|_\infty &\leq (1+\tilde{C}\Delta t)^s \left(\|\boldsymbol{e}_{n+1}\|_\infty + Csh_0 e^{-\frac{M^2h_0^2}{2}}\right) \\ &\leq (1+\tilde{C}\Delta t)^{(N_t-n)s}\|\boldsymbol{e}_{N_t}\|_\infty + Csh_0 e^{-\frac{M^2h_0^2}{2}} \sum_{i=1}^{N_t-n}(1+\tilde{C}\Delta t)^{is} \\ &\leq \frac{C_2 h_0}{\Delta t} e^{-\frac{M^2h_0^2}{2}} \left(e^{\tilde{C}s(T-t_n)}-1\right),\end{aligned}$$

where the constant $C_2 = C/\tilde{C}$. □

By combining Theorems 3.2 and 4.4, we now give the error estimate of the fully discrete SRK scheme (4.11). Let $\boldsymbol{u}(t_n)$ be the restriction of $u(t,\boldsymbol{x})$ on the mesh D_h and we obtain the following theorem.

Theorem 4.5. *Let $u(t,\boldsymbol{x})$ be the exact solution of* (1.1) *with $u \in C_b^{p+1,2p+2}$, and $\boldsymbol{u}_n$ be the numerical solution obtained from the fully discrete SRK scheme* (4.11) *with $\boldsymbol{u}_{N_t} = \boldsymbol{u}(T)$. Assume that $\|\varphi\|_{L^\infty} \leq \rho, Mh_0 > 1$ and $\{h_{ij}\}$ are sufficiently small. Then under the conditions in Theorem* 3.1, *we have*

$$\|\boldsymbol{u}(t_n) - \boldsymbol{u}_n\|_\infty \leq \left(e^{\tilde{C}s(T-t_n)}-1\right)\left(C_1(\Delta t)^p + \frac{C_2 h_0}{\Delta t} e^{-\frac{M^2h_0^2}{2}}\right),$$

where $\tilde{C} = \max_{|\xi|\leq\rho}|f'(\xi)|$ and the two positive constants C_1 and C_2 are independent of Δt and h_0.

Remark 4.3. The error estimate in (4.26) shows that the fully discrete SRK scheme can achieve exponential order convergence rate in space. To be more specific, we set Δt and Δx to satisfy $\Delta x/\sqrt{\Delta t} = \sigma_0/2$ and thus

$$h_0 = \frac{\Delta x}{\sigma_0\sqrt{\Delta t}} = \frac{1}{2}.$$

Then by (4.26), the spatial error of the scheme is about $\mathcal{O}(\exp(-M^2/8)/\Delta t)$, which decays in an exponential speed with respect to M^2. Thus, the spatial error of the fully discrete SRK scheme behaves like the one of spectral method, which is also convergent with exponential order.

5 Numerical experiments

To validate our theoretical results, we consider the reaction-diffusion equation in the backward form

$$u_t+\epsilon^2\Delta u+f(u)=0, \quad \boldsymbol{x}\in D=(0,1)^d, \quad t\in[0,T) \tag{5.1}$$

with the terminal condition $u(T,\boldsymbol{x})=\varphi(\boldsymbol{x})$ and subject to the periodic boundary condition. In this case, we have

$$\sigma=\sqrt{2}\epsilon,$$

and thus, by (4.12) and (4.24), we obtain the parameters $\{h_{ij}\}$ and h_0 as

$$h_{ij}=\frac{\Delta x}{\epsilon\sqrt{2(c_i-c_j)\Delta t}}, \quad h_0=\frac{\Delta x}{\epsilon\sqrt{2\Delta t}}.$$

In our tests, we set Δt and Δx to satisfy $\Delta x/(\epsilon\sqrt{\Delta t})=1/\sqrt{2}$ to get $h_0=1/2$ and $h_{ij}=1/(2\sqrt{c_i-c_j})$.

It is well known that the Eq. (5.1) can be seen as the L^2 gradient flow of the energy functional

$$E(u)=\int_D\left(\frac{\epsilon^2}{2}|\Delta u|^2+F(u)\right)d\boldsymbol{x}, \tag{5.2}$$

where $F(u)$ is a given potential function with $F'(u)=-f(u)$. Hence, the solution $u(t,\cdot)$ of (5.1) decreases the energy (5.2) when t decreases from T to 0, which is the so called energy dissipation law. In our tests, we will show that the proposed fully discrete SRK schemes can preserve this dissipation law.

We point out that we plotted Figs. 2, 3, 5, 6 and 8 in the backward order in the following subsections, where the abscissa from left to right is the values of $T-t$ with t decreasing from T to 0 or to a certain value smaller than T (e.g. to $T-20$ in Fig. 2). Moreover, all the figures in the numerical experiments section in our previous work [35] were also plotted in such a backward order.

5.1 Convergence tests

In this subsection, we test the convergence rates of the fully discrete SRK schemes (4.16)-(4.21). To this end, we set $\epsilon=0.1$ and consider the Ginzburg-Landau potential, i.e.

$$f(u)=u-u^3. \tag{5.3}$$

We take $T=1.0$ and choose the terminal condition as

$$\varphi(x,y)=0.1\big(\sin(2\pi x)\cos(2\pi y)+1\big).$$

To compute the errors, we regard the solution obtained by the SRK4 scheme (4.19) with $\Delta t=1/(2\times 40^2)$ and $M=30$ as the benchmark.

First, we test the convergence with respect to the quadrature number M. Since $h_0=1/2$, the estimate in (4.26) shows that the theoretical spatial error is about

$$\mathcal{O}\Big(e^{-\frac{(Mh_0)^2}{2}}\Big)=\mathcal{O}\Big(e^{-\frac{M^2}{8}}\Big). \tag{5.4}$$

Now we fix $\Delta t=1/(2\times 16^2)$ and calculate the numerical solutions of the SRK4 scheme at the time $t=0$ with $M=5,6,\ldots,20$. The numerical errors in the maximum-norm sense are presented in Fig. 1, which is clearly observed that the convergence rates with respect to M^2 are exponential order as shown in (5.4). It is also seen that when $Mh_0>7$, the errors remain almost the same, which is consistent with the conclusions in [38]. Thus, we shall always take $M=20$ (so that $Mh_0=10>7$) in the following tests to guarantee enough spatial accuracy.

Second, by setting $M=20$, we test the convergence in time. We calculate the numerical solutions of the schemes (4.16)-(4.21) at $t=0$ with various time step sizes $\Delta t=1/(2k^2)$ for $k=2,4,\ldots,16$. For comparison purpose, we compute the numerical solutions of the exponential time differencing Runge-Kutta (ETDRK) schemes up to second-order proposed in [9] and the IFRK schemes up to fourth-order constructed in [20] with the same time steps, where the central finite difference method with $\Delta x=1/128$ is adopted for the spatial discretization. The maximum norms of the numerical errors and corresponding convergence rates are listed in Tables 1-4, where the theoretical temporal convergence

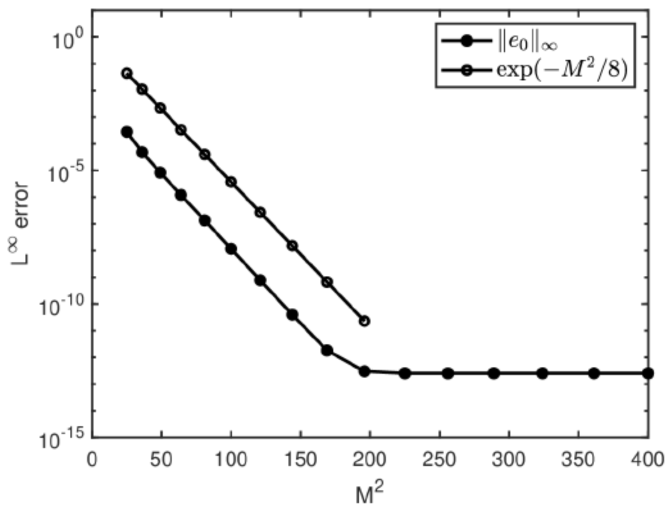

Figure 1: Evolutions of the errors of the SRK4 scheme with respect to M^2.

Table 1: Errors and convergence rates of the first-order schemes.

N_t	SRK1		ETDRK1		IFRK1	
	Error	Rate	Error	Rate	Error	Rate
2×2^1	1.523E-02	0.000	1.298E-02	0.000	1.523E-02	0.000
2×2^2	1.523E-02	0.000	1.298E-02	0.000	1.523E-02	0.000
2×4^2	3.983E-03	0.968	3.496E-03	0.946	3.983E-03	0.968
2×6^2	1.785E-03	0.990	1.576E-03	0.982	1.785E-03	0.990
2×8^2	1.007E-03	0.995	8.912E-04	0.991	1.007E-03	0.995
2×10^2	6.454E-04	0.997	5.717E-04	0.995	6.454E-04	0.997
2×12^2	4.485E-04	0.998	3.975E-04	0.997	4.485E-04	0.998
2×14^2	3.297E-04	0.999	2.923E-04	0.998	3.297E-04	0.999
2×16^2	2.525E-04	0.999	2.239E-04	0.998	2.525E-04	0.999

Table 2: Errors and convergence rates of the second-order schemes.

N_t	SRK2		ETDRK2		IFRK2	
	Error	Rate	Error	Rate	Error	Rate
2×2^2	6.307E-04	0.000	5.388E-04	0.000	6.307E-04	0.000
2×4^2	4.221E-05	1.951	3.613E-05	1.949	4.221E-05	1.951
2×6^2	8.444E-06	1.984	7.232E-06	1.984	8.444E-06	1.984
2×8^2	2.684E-06	1.992	2.299E-06	1.992	2.684E-06	1.992
2×10^2	1.101E-06	1.995	9.437E-07	1.995	1.101E-06	1.995
2×12^2	5.318E-07	1.997	4.556E-07	1.997	5.318E-07	1.997
2×14^2	2.872E-07	1.998	2.461E-07	1.998	2.872E-07	1.998
2×16^2	1.684E-07	1.998	1.443E-07	1.998	1.684E-07	1.998

Table 3: Errors and convergence rates of the third-order schemes.

N_t	SRK3		SRK3-I		IFRK3	
	Error	Rate	Error	Rate	Error	Rate
2×2^2	1.301E-05	0.000	1.175E-05	0.000	1.301E-05	0.000
2×4^2	2.183E-07	2.949	1.964E-07	2.952	2.183E-07	2.949
2×6^2	1.942E-08	2.984	1.746E-08	2.985	1.942E-08	2.984
2×8^2	3.471E-09	2.992	3.123E-09	2.992	3.472E-09	2.992
2×10^2	9.112E-10	2.997	8.217E-10	2.991	9.122E-10	2.995
2×12^2	3.049E-10	3.002	2.774E-10	2.978	3.058E-10	2.997
2×14^2	1.207E-10	3.007	1.130E-10	2.914	1.213E-10	2.998
2×16^2	5.414E-11	3.000	5.570E-11	2.647	5.447E-11	3.000

Table 4: Errors and convergence rates of the fourth-order schemes.

N_t	SRK4		SRK4-I		IFRK4	
	Error	Rate	Error	Rate	Error	Rate
2×2^2	5.040E-07	0.000	5.040E-07	0.000	5.040E-07	0.000
2×4^2	2.073E-09	3.963	2.073E-09	3.963	2.073E-09	3.963
2×6^2	8.143E-11	3.992	8.143E-11	3.992	8.142E-11	3.992
2×8^2	7.958E-12	4.042	7.958E-12	4.042	7.956E-12	4.042
2×10^2	1.184E-12	4.269	1.183E-12	4.272	1.176E-12	4.284
2×12^2	4.363E-13	2.739	4.367E-13	2.732	4.673E-13	2.530
2×14^2	2.920E-13	1.303	2.952E-13	1.270	3.495E-13	0.942
2×16^2	2.537E-13	0.526	2.549E-13	0.550	3.187E-13	0.346

rates are obviously observed. Moreover, the SRK schemes (4.16)-(4.21) can achieve the same accuracy as the ETDRK and IFRK schemes with the same convergence rates.

5.2 MBP preservation and energy stability

In this subsection, we test the MBP-preserving and energy-decreasing properties of the fully discrete SRK schemes. To this end, we use the schemes (4.16)-(4.21) to simulate the processes of the coarsening dynamics with $\epsilon=0.01$ and $T=1000$ for the Flory-Huggins potential with

$$f(u)=\frac{\theta}{2}\ln\frac{1-u}{1+u}+\theta_c u, \quad \theta=0.8, \quad \theta_c=1.6. \tag{5.5}$$

In our simulations, we take the uniform time step size $\Delta t=1/(2\times 2^2)$, then the spatial mesh size is obtained as $\Delta x=\epsilon\sqrt{\Delta t/2}=0.0025$. The terminal data is generated by the uniform distribution on $(-0.8,0.8)$. We plot the evolutions of the maximum norms of the numerical solutions in Fig. 2, where the red dash horizontal line shows the theoretical upper bound $\rho\approx 0.9575$ of the numerical solutions. We observe that the maximum norms of the numerical solutions are all bounded by the theoretical value, which suggests that the schemes preserve the MBP. Fig. 3 plots the evolutions of the energies of the numerical solutions, which show that the schemes inherit the energy dissipation law.

In addition, we present in Fig. 4 the evolution of the phase structures at $T-t=4$, 6,10,100,350, and 660 generated by the SRK4 scheme, respectively. It is seen that the simulated dynamics begins with a random state and towards the homogeneous steady state of constant ρ, which is reached after about $T-t=689$ in our simulation. The evolutions of the phase structures generated by the other SRK schemes are similar to the one of the SRK4 scheme.

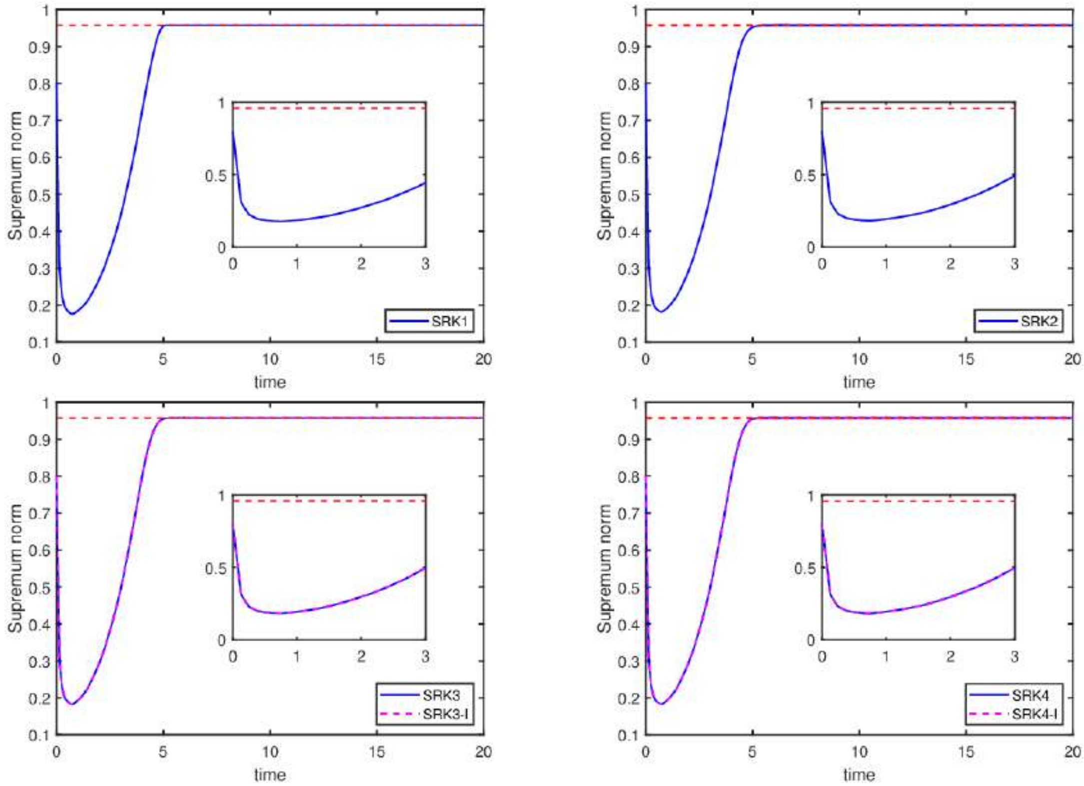

Figure 2: Evolutions of the supremum norms of the SRK schemes.

5.3 Comparison for third-order schemes

In this subsection, we illustrate the importance of MBP-preserving schemes. To this end, we solve the Eq. (5.1) with the Flory-Huggins potential using two different third-order schemes, that is, the SRK3 scheme (4.18) and the IFRK3 Shu-Osher scheme considered in [20,27] (see [20, Scheme (29)] or [27, Scheme (6.2)]). Since the essential condition $c_i \geq c_j$ for $i \geq j$ is not satisfied, the IFRK3 Shu-Osher scheme may not preserve the MBP.

We set $\epsilon = 0.1$ and $T = 20$. A random terminal data is generated by the uniform distribution on $(-0.8, 0.8)$. For the SRK3 scheme, we take $\Delta t = 1/72$ and $\Delta x = 1/120$. As for the IFRK3 Shu-Osher scheme, we take $\Delta t = 1/200$ and $\Delta x = 1/512$.

Fig. 5 presents the evolutions of the maximum norm and the energy of the numerical solutions of the SRK3 scheme, where the MBP is perfectly preserved and the energy decreases monotonically along the time. Fig. 6 gives the evolutions of the maximum norm and the energy of the numerical solutions of the IFRK3 Shu-Osher scheme, which clearly show that the IFRK3 Shu-Osher scheme does not preserve the MBP and the energy dissipation law even for a small time step size. Although the IFRK3 Shu-Osher scheme may preserve the MBP when the time step size is small enough, there is no theoretical proof for now.

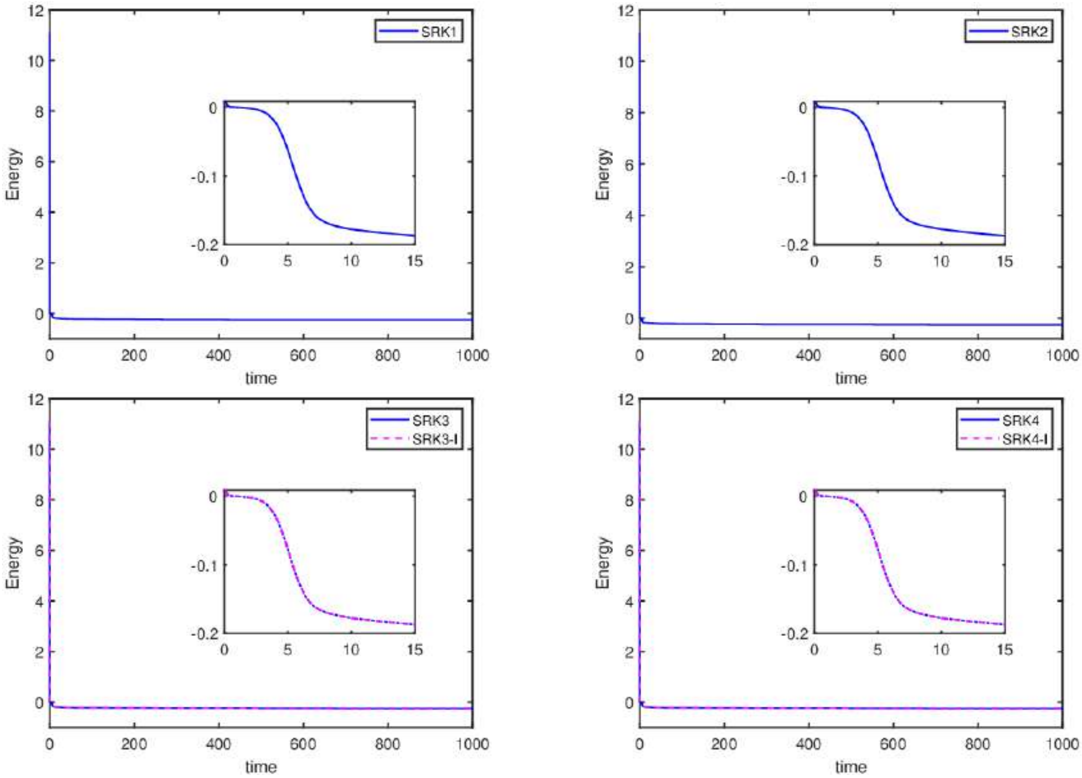

Figure 3: Evolutions of the energies of the SRK schemes.

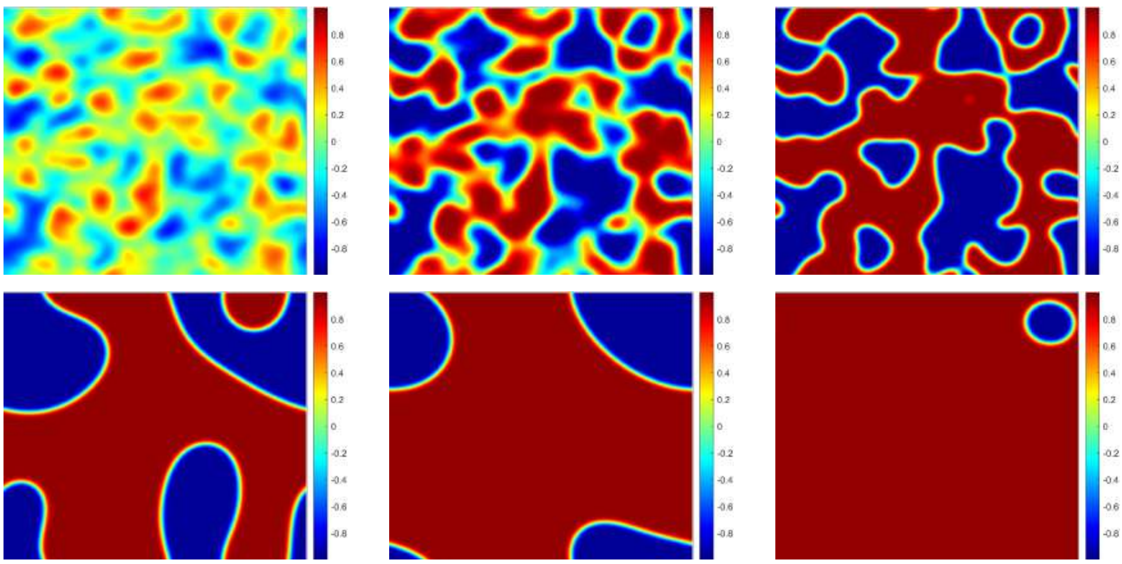

Figure 4: Evolution of the phase structure obtained by using the SRK4 scheme. From left to right and from top to bottom: $T-t=4,6,10,100,350$, and 660.

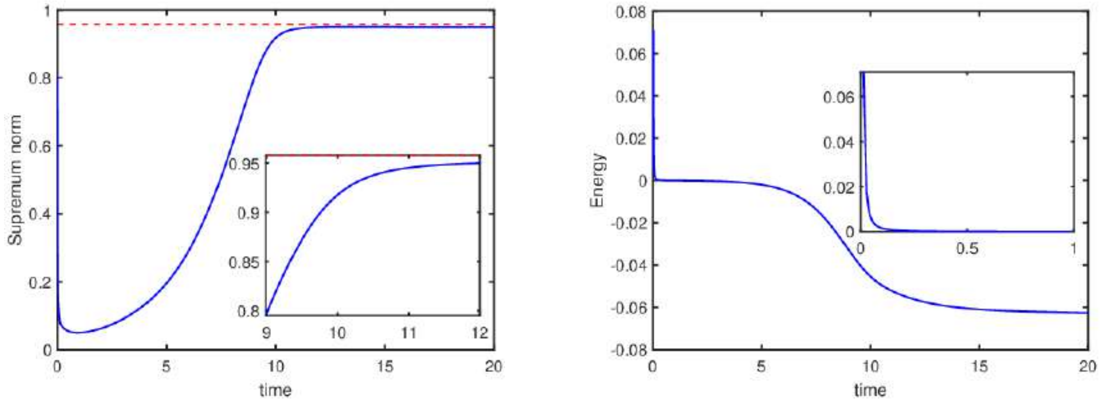

Figure 5: Evolutions of the supremum norm (left) and the energy (right) for the SRK3 scheme.

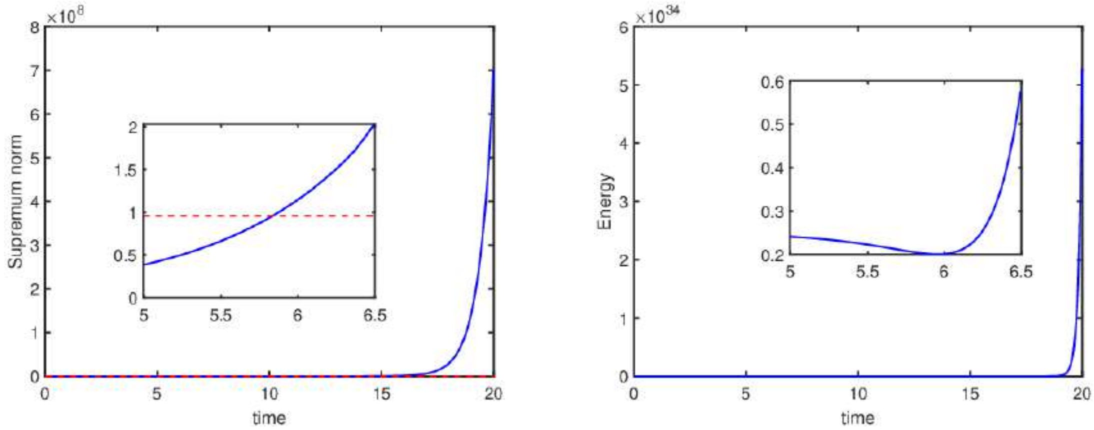

Figure 6: Evolutions of the supremum norm (left) and the energy (right) for the IFRK3 Shu-Osher scheme.

5.4 3D coarsening dynamics

In this subsection, we consider the simulation of the 3D coarsening dynamics of the Eq. (5.1) for the Flory-Huggins potential with $\epsilon=0.02$ and $T=500$. In our simulation, we take the time step size $\Delta t=1/(2\times 2^2)$ and the corresponding mesh size $\Delta x=0.005$.

We use the SRK4 scheme to simulate the 3D coarsening dynamics with a random terminal data ranging from -0.8 to 0.8. Fig. 7 presents the evolution of the zero-isosurface of the numerical solutions at $T-t=1,10,100,200,300$, and 330, respectively. Similar to the 2D case, the simulated dynamics begins with a random state and reaches the steady state of constant ρ around $T-t=336$. Fig. 8 gives the evolutions of the maximum norm and the energy of the numerical solutions. It is seen again that the MBP is perfectly preserved and the energy decreases monotonically along the time.

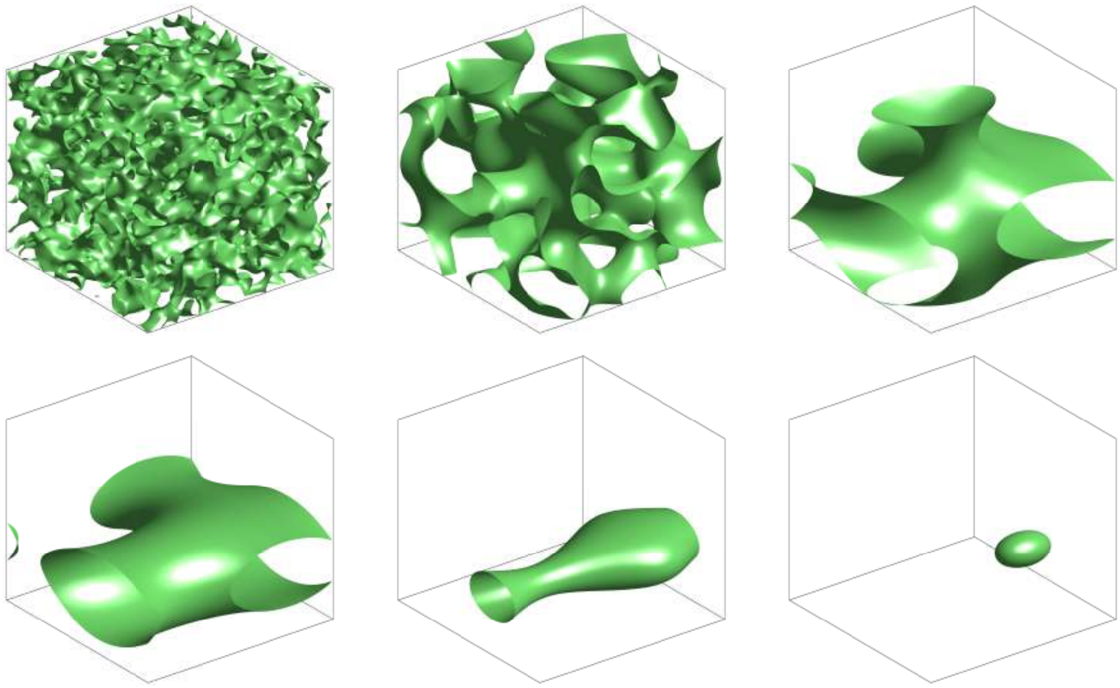

Figure 7: The snapshots of the evolution at $T-t=1,10,100,200,300,330$, respectively (left to right and top to bottom), for the 3D coarsening dynamics.

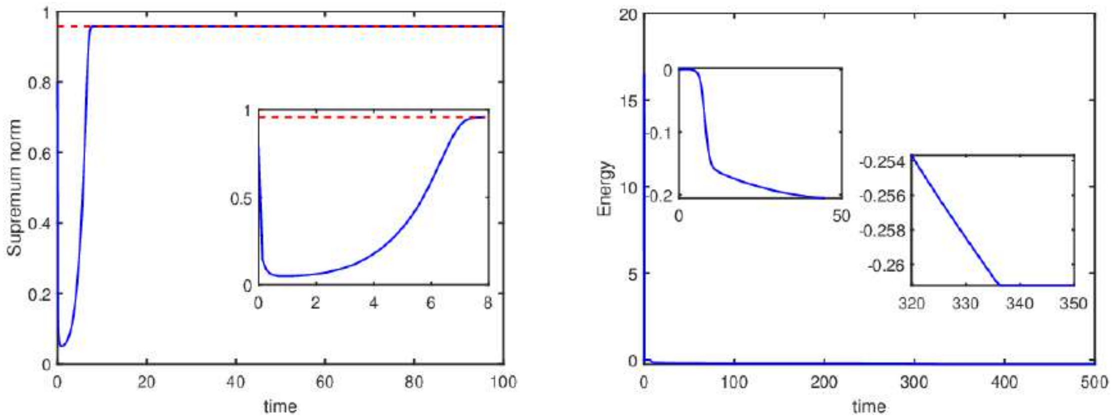

Figure 8: Evolutions of the supremum norm (left) and the energy (right) for the 3D coarsening dynamics.

6 Conclusions

We proposed and analyzed a class of high-order fully discrete MBP-preserving SRK schemes for solving the semilinear parabolic equations by using the Sinc quadrature rule to approximate the conditional expectations in the time semidiscrete SRK schemes developed in the first part of this series. We established their error estimates rigorously, which show that the proposed schemes can achieve exponential order accuracy in space. Particularly, we constructed several specific fully discrete MBP-preserving SRK schemes with up to fourth-order accuracy in time. In addition, by analyzing the eigenvalues of the conditional expectation operator in SRK method and the exponential Laplacian operator in IFRK method under the periodic boundary condition, we revealed the equivalence of the time semidiscrete SRK and IFRK methods. Some numerical experiments were carried out to verify the theoretical results and to validate the exponential order convergence rate in space of the proposed fully discrete schemes.

Acknowledgments

The authors would like to thank the anonymous reviewers for their valuable suggestions, which helped us to improve this article greatly.

This work was partially supported by the NSF of China (Nos. 12071261, 12371398, 12001539, 11831010), by the national key R&D Program of China (No. 2018YFA0703900), and by the China Postdoctoral Science Foundation (No. 2019TQ0073).

References

[1] P. Briand and R. Carmona, *BSDEs with polynomial growth generators*, J. Appl. Math. Stochastic Anal., 13:207–238, 2020.

[2] E. Burman and A. Ern, *Stabilized Galerkin approximation of convection-diffusion-reaction equations: Discrete maximum principle and convergence*, Math. Comp., 74:1637–1652, 2005.

[3] P. Chatzipantelidis, Z. Horvath, and V. Thomee, *On preservation of positivity in some finite element methods for the heat equation*, Comput. Methods Appl. Math., 15:417–437, 2015.

[4] W. Chen, C. Wang, X. Wang, and S. Wise, *Positivity-preserving, energy stable numerical schemes for the Cahn-Hilliard equation with logarithmic potential*, J. Comput. Phys. X, 3:100031, 2019.

[5] P. Ciarlet, *Discrete maximum principle for finite-difference operators*, Aequationes Math., 4:338–352, 1970.

[6] P. Ciarlet and P. Raviart, *Maximum principle and uniform convergence for the finite element method*, Comput. Methods Appl. Mech. Engrg., 2:17–31, 1973.

[7] J. Cui, D. Hou, and Z. Qiao, *Energy regularized models for logarithmic SPDEs and their numerical approximations*, arXiv:2303.05003, 2023.

[8] Q. Du, L. Ju, X. Li, and Z. Qiao, *Maximum principle preserving exponential time differencing schemes for the nonlocal Allen-Cahn equation*, SIAM J. Numer. Anal., 57:875–898, 2019.

[9] Q. Du, L. Ju, X. Li, and Z. Qiao, *Maximum bound principles for a class of semilinear parabolic equations and exponential time differencing schemes*, SIAM Rev., 63:317–359, 2021.

[10] Z. Fu, T. Tang, and J. Yang, *Energy plus maximum bound preserving Runge-Kutta methods for the Allen-Cahn equation*, J. Sci. Comput., 92:97, 2022.

[11] Z. Fu, T. Tang, and J. Yang, *Energy diminishing implicit-explicit Runge-Kutta methods for gradient flows*, Math. Comput., 2024. doi: 10.1090/mcom/3950.

[12] Z. Fu and J. Yang, *Energy-decreasing exponential time differencing Runge-Kutta methods for phase-field models*, J. Comput. Phys., 454:110943, 2022.

[13] D. Hou, L. Ju, and Z. Qiao, *A linear second-order maximum bound principle-preserving BDF scheme for the Allen-Cahn equation with a general mobility*, Math. Comput., 92:2515–2542, 2023.

[14] T. Hou and H. Leng, *Numerical analysis of a stabilized Crank-Nicolson/Adams-Bashforth finite difference scheme for Allen-Cahn equations*, Appl. Math. Lett., 102:106150, 2020.

[15] T. Hou, T. Tang, and J. Yang, *Numerical analysis of fully discretized Crank-Nicolson scheme for fractional-in-space Allen-Cahn equations*, J. Sci. Comput., 72:1214–1231, 2017.

[16] T. Hou, D. Xiu, and W. Jiang, *A new second-order maximum-principle preserving finite difference scheme for Allen-Cahn equations with periodic boundary conditions*, Appl. Math. Lett., 104:106265, 2020.

[17] J. Huang, L. Ju, and Y. Xu, *Efficient exponential integrator finite element method for semilinear parabolic equations*, SIAM J. Sci. Comput., 45:A1545–A1570, 2023.

[18] L. Ju, X. Li, and Z. Qiao, *Stabilized exponential-SAV schemes preserving energy dissipation law and maximum bound principle for the Allen-Cahn type equations*, J. Sci. Comput., 92:66, 2022.

[19] L. Ju, X. Li, and Z. Qiao, *Generalized SAV-exponential integrator schemes for Allen-Cahn type gradient flows*, SIAM J. Numer. Anal., 60:1905–1931, 2022.

[20] L. Ju, X. Li, Z. Qiao, and J. Yang, *Maximum bound principle preserving integrating factor Runge-Kutta methods for semilinear parabolic equations*, J. Comput. Phys., 439:110405, 2021.

[21] N. Karoui, S. Peng, and M. Quenez, *Backward stochastic differential equations in finance*, Math. Finance, 7:1–71, 1997.

[22] B. Li, J. Yang, and Z. Zhou, *Arbitrarily high-order exponential cut-off methods for preserving maximum principle of parabolic equations*, SIAM J. Sci. Comput., 42:3957–3978, 2020.

[23] J. Li, R. Lan, Y. Cai, L. Ju, and X. Wang, *Second-order semi-Lagrangian exponential time differencing method with enhanced error estimate for the convective Allen-Cahn equation*, J. Sci. Comput., 97:7, 2023.

[24] J. Li, X. Li, L. Ju, and X. Feng, *Stabilized integrating factor Runge-Kutta method and unconditional preservation of maximum bound principle*, SIAM J. Sci. Comput., 43:A1780–A1802, 2021.

[25] J. Lund and K. Bowers, *Sinc Methods for Quadrature and Differential Equations*, SIAM, 1992.

[26] L. Ma and Z. Qiao, *An energy stable and maximum bound principle preserving scheme for the dynamic Ginzburg-Landau equations under the temporal gauge*, SIAM J. Numer. Anal., 61:2695–2717, 2023.

[27] C. Nan and H. Song, *The high-order maximum-principle-preserving integrating factor Runge-Kutta methods for nonlocal Allen-Cahn equation*, J. Comput. Phys., 456:111028, 2022.

[28] É. Pardoux, *BSDEs, weak convergence and homogenization of semilinear PDEs*, in: Nonlinear Analysis, Differential Equations and Control. Nato Science Series C, Vol. 528, Springer, 503–549, 1999.

[29] É. Pardoux and S. Peng, *Adapted solution of a backward stochastic differential equation*, Systems Control Lett., 14:55–61, 1990.

[30] G. Peng, Z. Gao, and X. Feng, *A stabilized extremum-preserving scheme for nonlinear parabolic equation on polygonal meshes*, Internat. J. Numer. Methods Fluids, 90:340–356, 2019.

[31] G. Peng, Z. Gao, W. Yan, and X. Feng, *A positivity-preserving nonlinear finite volume scheme for radionuclide transport calculations in geological radioactive waste repository*, Int. J. Numer. Methods Heat Fluid Flow, 30:516–534, 2019.

[32] S. Peng, *Probabilistic interpretation for systems of quasilinear parabolic partial differential equations*, Stochastics Stochastics Rep., 37:61–74, 1991.

[33] J. Shen, T. Tang, and J. Yang, *On the maximum principle preserving schemes for the generalized Allen-Cahn equation*, Commun. Math. Sci., 14:1517–1534, 2016.

[34] F. Stenger, *Handbook of Sinc Numerical Methods*, CRC Press, 2016.

[35] Y. Sun and W. Zhao, *Stochastic Runge-Kutta methods for preserving maximum bound principle of semilinear parabolic equations. Part I: Gaussian quadrature rule*, CSIAM Trans. Appl. Math., 5:390–420, 2024.

[36] T. Tang and J. Yang, *Implicit-explicit scheme for the Allen-Cahn equation preserves the maximum principle*, J. Comput. Math., 34:471–481, 2016.

[37] R. Varga, *On a discrete maximum principle*, SIAM J. Numer. Anal., 3:355–359, 1966.

[38] X. Wang, W. Zhao, and T. Zhou, *Sinc-θ schemes for backward stochastic differential equations*, SIAM J. Numer. Anal., 60:1799–1823, 2022.

[39] X. Xiao, Z. Dai, and X. Feng, *A positivity preserving characteristic finite element method for solving the transport and convection-diffusion-reaction equations on general surfaces*, Comput. Phys. Commun., 247:106941, 2020.

[40] X. Xiao, X. Feng, and Y. He, *Numerical simulations for the chemotaxis models on surfaces via a novel characteristic finite element method*, Comput. Math. Appl., 78:20–34, 2019.

[41] J. Yang, Z. Yuan, and Z. Zhou, *Arbitrarily high-order maximum bound preserving schemes with cut-off postprocessing for Allen-Cahn equations*, J. Sci. Comput., 90:76, 2022.

[42] X. Yang, *Error analysis of stabilized semi-implicit method of Allen-Cahn equation*, Discrete Contin. Dyn. Syst. Ser. B, 11:1057–1070, 2009.

[43] W. Zhao, W. Zhang, and L. Ju, *A numerical method and its error estimates for the decoupled forward-backward stochastic differential equations*, Commun. Comput. Phys., 15:618–646, 2014.